Chapter 1

# Background, Motivation, and Overview

1.1 INTRODUCTION

The word "university" is derived from the word "universal" (Newman, 1927) in that the university is the foremost setting for teaching universal knowledge. Philosophy, chemistry, agriculture, mechanics, theology, biology, and so on are all topics of learning, teaching, and exploring at the true university. The study of vibrations is a microcosm of the ideal university, encompassing aspects of dynamics, fluid mechanics, structural deformation and fatigue, electromagnetism, feedback control, sound, and other phenomena. Confronting this, the eager investigator feels great satisfaction in drawing ideas from each area and then forging solutions to vibration problems. As an athlete develops calves and biceps, shoulders, and forearms and then enjoys using these in harmony and mutual support in competition, so the vibration engineer delights in recognizing and using many disciplines to tame vibrations.

With its arsenal of anomalies—fastener looseness, structural member fatigue and failure, noise, internal rubs in machinery, human fatigue and distractions, optical instrumentation and machining errors, and so on—vibration continues to present formidable engineering challenges and to limit energy efficiency and cost reduction in machinery and structures in the twenty-first century. New machinery that pushes the envelopes of efficiency and power density; new structures that stretch the imagination in size, materials, light weights, and locations; and new vehicles that propel us through land, air, sea, and space with ever increasing speed and comfort level all hold great promise for an efficient and convenient future. These advances will come at a price though and vibration will be there to collect its due. *The author extends his best wishes for success to those who meet the vibration challenges that continue to arise in mankind's quest to subdue nature and use its awesome forces for peace, human dignity, and prosperity.*

1.2 BACKGROUND

The following sections provide discussions of many important aspects of vibration. The intent of this section is to provide some basic background material to facilitate understanding of the following sections. Vibration is the study of dynamic motions of mechanical, structural, or anatomical components or systems about their static equilibrium configurations. The motion may be sinusoidal periodic, complex periodic, quasiperiodic, transient, chaotic, or random. Monotone (single-frequency) sinusoidal vibration is characterized by an equilibrium position x_{eq} and the dynamic displacement *amplitude* (A_x), *phase angle* (ϕ_x), *frequency* (f), and *period* (T) as shown in Figure 1.2.1.
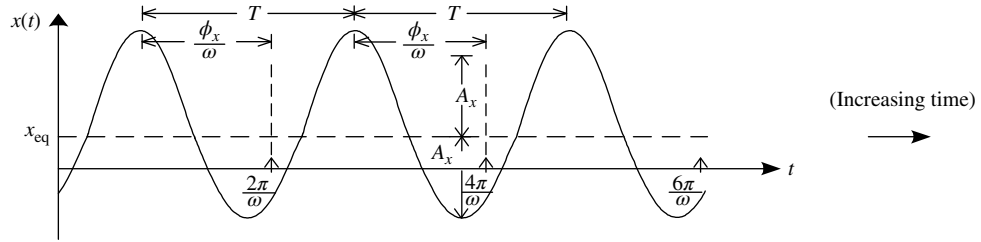
Figure 1.2.1 Pure tone sinusoidal vibration

The period and frequency are related by

$$f = \frac{1}{T} \text{ cycles/s or Hz}, \quad \omega = 2\pi f \text{ circular frequency in rad/s} \tag{1.2.1}$$

Period markers are seen to occur at $0, 2\pi/\omega, 4\pi/\omega, \dots$. This may represent a once per revolution event on a rotating shaft or just some arbitrarily referenced pulse that indicates the beginning of a new forcing period. The motion is described using the expression

$$x(t) = A_x \cos(\omega t + \phi_x) \tag{1.2.2}$$

The positive peaks occur when the argument of the cosine function is a multiple of 2π, that is,

$$\omega t_{pn} + \phi_x = 2\pi n \quad n = 1, 2, \dots \tag{1.2.3}$$

which implies

$$t_{pn} \in \left\{ \frac{2\pi}{\omega} - \frac{\phi_x}{\omega}, \frac{4\pi}{\omega} - \frac{\phi_x}{\omega}, \frac{6\pi}{\omega} - \frac{\phi_x}{\omega}, \dots \right\} \tag{1.2.4}$$

Thus, it is seen by comparison of (1.2.4) and Figure 1.2.1 that the phase angle ϕ_x has a physical interpretation, namely, it provides a measure of the time between $x(t)$ experiencing a positive peak and the occurrence of a period marker. This time lag is

$$\Delta t_p = \frac{\phi_x}{\omega} \tag{1.2.5}$$

The velocity and acceleration expressions are obtained by differentiating (1.2.2)

$$v(t) = \dot{x}(t) = A_v \cos(\omega t + \phi_v) \tag{1.2.6}$$

$$a(t) = \dot{v}(t) = \ddot{x}(t) = A_a \cos(\omega t + \phi_a) \tag{1.2.7}$$

where

$$\begin{aligned} A_v &= \omega A_x, & \phi_v &= \phi_x + \frac{\pi}{2} \\ A_a &= \omega A_v = \omega^2 A_x, & \phi_a &= \phi_v + \frac{\pi}{2} = \phi_x + \pi \end{aligned} \tag{1.2.8}$$

The motion depicted in Figure 1.2.1 could result from displacing or striking the component and allowing it to freely vibrate as in the case of a swing, traffic light, car antenna,

cantilevered ruler, bell, or guitar string. The frequency of this natural or "free" motion is called a "natural frequency." Alternatively, the motion could result from being forced by some source that has a frequency ω, as in the case of a washing machine with an unbalanced load, a vehicle with a slightly oval tire, or an offshore platform subjected to periodic wave forces at frequency ω. The oval tire would actually induce a vibration at frequency 2ω if its rotation frequency is ω.

So what happens if the forcing (source) frequency nearly equals the structural component's natural frequency? The answer is that the vibration may become very large and even cause failure of the component. This phenomenon is called *resonance*, and it was a major reason for the spectacular failure of the Tacoma Bridge in Washington, United States, on November 7, 1940. Many years later, resonance still persists as a common source of failure for many structures and machines. An explanation for the increase in vibration amplitude at resonance accentuates a major distinction between static deflection and dynamic motion, namely, the existence of an *inertial force*. The *stiffness* force in a component is proportional to its deflection and acts to restore it to its equilibrium state when deflected. The inertial force is proportional to acceleration which is 180° out of phase with the displacement as shown by (1.2.8). The inertial force may become large and cancel the restoring stiffness force. This causes the dynamic motion (vibration) to become very large and destructive. This simplified example of resonance is extended to complex systems in Chapter 7.

Free (unforced) vibration decays with time due to energy dissipating forces such as:

- Viscous, dry, or atmospheric friction
- Material hysteresis
- Eddy current generated magnetic forces of an electrically conductive component that vibrates in a magnetic field

This vibration decay is illustrated in Figure 1.2.2. The presence of the *damping* force prevents exact cancellation of the stiffness restoring force by the inertial force at resonance. This, and nonlinear effects, reduces the infinite amplitude, resonant vibrations to finite values. Thus, damping is generally good for attenuating resonant vibrations. As with most things in life though, too much of a good thing may be bad, and damping is no exception. The velocity at the point where a viscous damper is attached to a flexible body will become zero as the damper strength increases. The energy dissipated by the damper is proportional to the square of the velocity of the attachment point. Therefore, very little energy is dissipated and all other points on the flexible body may vibrate severely. Thus, an optimum level of damping is sought in practice.

Systems may vibrate with many *free and/or forced frequencies* simultaneously. This results because:

- Actual components such as buildings, piping systems, shafts, blades, guitar strings, and so on have many natural frequencies.
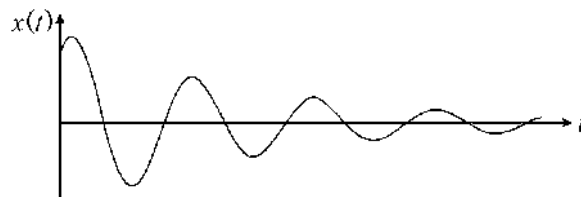
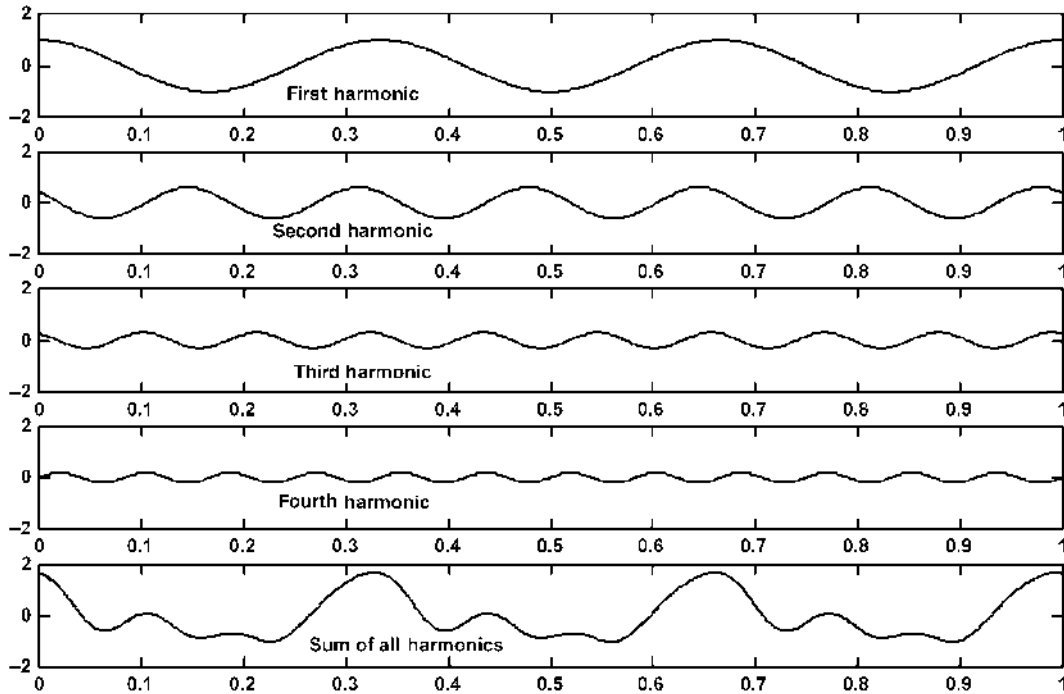**Figure 1.2.2** Damped free vibrations

Figure 1.2.3 Lowest four constituent harmonics and their sum

- Some systems are excited by multiple sources at different frequencies. For example, a jet engine generally has two coaxial shafts: one a power turbine and the other a gas generator. Mass imbalances on the two shafts exert forces on the engine at the power turbine spin frequency and at the gas generator spin frequency.

- Some forces are periodic but not purely sinusoidal such as piston pressure or crankshaft/ connecting rod/piston inertial forces in a vehicle engine or reciprocating pump or compressor, or a jack hammer striking building flooring, and so on.

Multifrequency vibration is referred to generally as complex periodic and is illustrated by Figure 1.2.3. A *Fourier* series expansion (see Chapter 2) will reveal all of the amplitudes, phase angles, and frequencies of the constituent sine waves that are superimposed to form the complex waveform.

Some vibrations are not entirely periodic since these result from nonperiodic excitations such as step, impulse, ramp, or more general shock inputs. Finally, some excitations such as atmospheric buffeting of airplanes or helicopters may be random, which causes the responses also to be random. Complex and random vibration waveforms may display many sinusoidal components of varying amplitude and duration. A common measure of severity determined from these responses is the *root mean square (rms) value*

$$x_{\mathrm{rms}} = \sqrt{\frac{1}{T} \int_0^T x^2(t)\ dt} \qquad\qquad (1.2.9)$$

where T is the period of measurement. For single-frequency sinusoidal motion, (1.2.9) yields

$$x_{\text{rms}} = \sqrt{\frac{1}{T}\int_0^T [A_x \cos(\omega t + \phi_x)]^2 dt} = \frac{A_x}{\sqrt{2}} \tag{1.2.10}$$

where T is one cycle of the motion. For multiharmonic complex motion, (1.2.9) yields

$$x_{\text{rms}} = \sqrt{\frac{1}{T}\int_0^T [A_{x1}\cos(\omega t + \phi_{x1}) + A_{x2}\cos(2\omega t + \phi_{x2}) + \cdots + A_{xn}\cos(n\omega t + \phi_{xn})]^2 dt}$$

$$= \sqrt{\frac{1}{2}\left(A_{x1}^2 + A_{x2}^2 + \cdots + A_{xn}^2\right)}$$

$$\tag{1.2.11}$$

where T equals the period of the lowest (fundamental) harmonic

$$T = \frac{2\pi}{\omega} \tag{1.2.12}$$

which is also the period of the complex, multiharmonic waveform.

1.2.1   Units

The vast majority of the units in this text are metric. Some helpful conversions are given below:

$1g$ (gravity constant) $= 9.81$ m/s^2 $= 386$ in./s^2 (on earth)

1 mil $= 0.001$ in. $= 0.0254$ mm $= 25.4$ μm

1 in. $= 0.254$ m $= 2.54$ cm $= 25.4$ mm

1 m $= 39.37$ in. $= 3.281$ ft

1 km $= 0.62$ miles

1 N $= 0.219$ lbf

1 lbf $= 4.54$ N

1 N/m $= 0.0056$ lb/in.

1 lb/in. $= 178.6$ N/m

1 N/m^2 $= 1$ Pa $= 1.42 \times 10^{-4}$ lb/in.^{2}

1 lb/in.^{2} $= 7032.3$ N/m^2

1 in.^{4} $= 4.162 \times 10^{-7}$ m^4

1 m^4 $= 2.403 \times 10^6$ in.^{4}

1 lb.s/in. $= 178.6$ N.s/m

1 N.s/m $= 0.0056$ lb.s/in.

1 in.lb/rad $= 0.1153$ N.m/rad

1 N.m/rad $= 8.672$ in.lb/rad

Weight of 1 kg $= 9.81$ N $= 2.161$ lbf (on earth)

1.3   OUR VIBRATING WORLD

The term vibration has many different connotations but is most often connected with oscillatory motion of an object about some equilibrium position and/or operating point. The Merriam-Webster dictionary entry for vibration provides a commendable description for the "vibrations" studied in this text, that is, "periodic motion of the particles of an elastic body or medium in alternately opposite directions from the position of equilibrium when that equilibrium has been disturbed (as when a stretched cord produces musical tones or molecules in the air transmit sounds to the ear)." A vibration engineer might add "a source of cyclic fatigue, looseness, human health or contact damage which limits the performance of machines and people."

Vibrations are often related to a natural frequency and resonance. Objects vibrate at certain characteristic frequencies due to the periodic exchange of energy between kinetic and potential forms. So bells, traffic lights, pendulums, car antennas, turbine blades, and so on sway and ring at certain frequencies when displaced and released. Resonance occurs when an excitation or disturbance acts on an object with nearly the same frequency as the object's natural frequency. The result may be large, damaging, and sometimes catastrophic vibrations.

1.3.1   Small-Scale Vibrations

The potential energy that is created when atoms are collected in a lattice produces forces that act like spring connecting the atoms. These masses connected by "springs" vibrate and are particularly sensitive to certain excitation frequencies referred to as resonance frequencies. Cesium 133 atoms have a resonant frequency at 9,192,631,770 cycles/s. When excited at this frequency, the atoms change state. A voltage applied to a piezoelectric crystal causes it to deform. The vibrating piezoelectric is utilized to create microwaves which impinge on the cesium atoms. If the frequency of the voltage varies near 9,192,631,770 Hz, the microwaves cause the cesium 133 to experience a peak in the number of transformed atoms as resonance occurs at the atomic natural frequency. These atoms are continuously counted as the frequency of the voltage applied to the piezoelectric is varied. A peak count indicates that the frequency is exactly 9,192,631,770 Hz (cesium 133 atomic resonant frequency). The cycles are counted and every 9,192,631,770 cycles form 1 second. Hence, vibrations even on the atomic level reveal a practical usage, that is, an *atomic clock*.

The lens-free atomic force microscope (AFM) employs a tiny 100 μm length cantilever beam to measure local sample height (topography) at the atomic level. The beam has a very low spring stiffness (0.1 N/m) yet very high natural frequency. Mounted on the end of the cantilever is a sharp tip that is typically a 3 μm tall pyramid with 10–30 nm end radius. The deflection of the tip is measured with a laser. The beam and tip may also function in a non-contact mode where topographic images are derived from measurements of attractive forces. Environmental vibration, that is, due to a passing truck, can cause severe distortion of the images produced by an AFM.

On a slightly larger scale, a tiny quartz crystal in a watch may vibrate (ring) for minutes similar to a tuning fork due to a lack of damping. Deflection of the quartz (piezoelectric) crystal creates a voltage that can be amplified and reapplied to the crystal to sustain the vibration at its "natural" frequency. This frequency is known and constant so a count of the number of cycles executed provides a means to determine the passing of 1 second—that is, the fundamental time unit for the watch.

Vibrations occur in the human body on a very small scale yet they are also very important. Consider the auditory system consisting of the external, middle, and inner ear. The

outer portion of the external ear (auricle) directs sound waves to the 2.5 cm long ear canal, passing to the ear drum (tympanic membrane). The ear drum is about 1 cm in diameter, has a concave shape, and vibrates in response to the incoming sound waves. Its displacement amplitude during normal speech (~60 dB sound level) is estimated to be about equal to the size of a molecule of hydrogen. The middle ear consists of three solid material "ossicles," the hammer (malleus), the anvil (incus), and the stirrup (stapes), which increase the vibratory force about 20 times as it is transmitted from the ear drum to the "oval window." This results from lever action of the ossicles and the decrease in area between the ear drum and oval window. The stapes displaces the oval window as it transmits the sound waves (vibration). This oval window acts as a piston oscillating the fluid (perilymph) within the snail-shaped cochlea which winds about 2¾ turns. The fluid causes the "basilar membrane" in the cochlea to vibrate in different manners according with the frequency of the exciting sound wave. Frequencies below 50 Hz cause vibration of the entire membrane, whereas higher frequencies (15–24 KHz) cause the membrane to vibrate only at its base attachment point. The membrane is covered with hair cells that move against a second membrane (tectorial). Microvilli (minute projections of cell membranes that greatly increase surface area) that are embedded in the tectorial membrane bend in response to movement of the basilar membrane. Bending of the microvilli causes ionic actions that stimulate nerves connected to the acoustic cortex in the brain, via the basilar hair cells. As mentioned, different frequencies cause different parts of the basilar membrane to deflect which in turn bends different microvilli, which in turn affect different nerves that synapse (membrane-to-membrane contact of two nerve cells that promotes transmission of nerve impulses) with the basilar hair cells. These nerves are connected to different positions along the acoustic cortex. Thus, the frequency of the sound waves determines which part of the basilar membrane vibrates, which tectorial membrane microvilli bend, which basilar membrane hairs synapse with nerves to the acoustic cortex, and which portion of the acoustic cortex is stimulated. The audible frequency range extends from 20 Hz to 24 KHz. For reference, the lowest frequency of a piano is 27.5 Hz and the highest is 4186 Hz. In addition, middle C is 400 Hz, and the next C is one octave (factor of 2) higher at 800 Hz. J. S. Bach divided each octave into 12 equal frequency intervals to include flats and sharps (Cannon, 1967). Each note is then $2^{1/12}$ (1.0595) higher in frequency than the next lower note. From this discussion, it is clear that the ear acts as a transduction device that converts vibrations into nerve impulses.

Small vibrations also occur in the vocal folds (chords) of the human throat. The left and right vocal folds are made of muscles and form a "V" when viewed from above. The folds are pulled apart from one another when breathing and are pulled together during speech. Talking, singing, and humming cause the two folds to open and close very quickly as air passes from the lungs through the windpipe and then through the folds. The folds are forced open by the higher air pressure in the windpipe but quickly close as the pressure decreases due to the escaping air. The windpipe pressure builds up again and the pattern is repeated at a high frequency. Thus, sound is produced as the small jets of air pass through the moving vocal folds. The shape of the vocal tract changes as the tongue, jaw, palate, and lips are moved. This causes the air in the voice tract to respond (resonate) at different frequencies (acoustic natural frequencies) to the vocal fold vibration and corresponding air jets. This is similar to blowing across the openings of several bottles that are filled to different levels with water, each producing a distinct pitch due to the difference in cavity shape. The lowest (fundamental) spoken frequency is about 100 Hz and the highest about 3000 Hz. Articulation is the action of changing the vocal tract geometry to produce desired sounds. Vowels resonate in the throat and consonants in the nasal passages.

1.3.2   Medium-Scale (Mesoscale) Vibrations

Trucks, autos, buses, trains, and amusement park rides bounce and buzz due to road or track unevenness and machinery forces developed in the engine, transmission, and auxiliary equipment. Airplanes shake and vibrate due to air turbulence and dynamic forces in their engines. The same scenario exists for helicopters with the addition of torque transmission-related dynamic forces for the main and tail rotor. Ships utilize many machines (turbines, gear boxes, propellers, pumps, ventilation fans, and so on) that cause vibration and also experience sea wave excitation. Industrial chemical, petroleum, paper product, and power plants utilize hundreds of compressors, turbines, pump, fans, and so on that vibrate due to rotating imbalance, misalignment, gear and blade forces, and so on and in turn excite many kilometers of attached piping and vessels. Mills, lathes, drill presses, and saws shake and vibrate due to imbalance and cutting forces in thousands of machine shops and manufacturing facilities. This may cause delirious effects on surface finish, and limit the depth and rate of cut, and consequently the tool performance. Buildings for the most part buzz and vibrate due to HVAC equipment and sway due to wind buffeting. Precision optical instruments such as lasers, telescopes, microscopes, and interferometers vibrate due to transmission of forces from neighboring machinery and forces, oftentimes degrading the instrument's performance. Musical instruments (strings and drums) vibrate but in a (hopefully) pleasant manner. Skis, baseball bats, tennis rackets, and golf clubs also vibrate in response to impact loading. These medium-scale vibrations typically occur with an amplitude range of 0.01–10.0 mm and a frequency range of 2–2000 Hz. These vibrations are rarely detectable with the naked eye but can have catastrophic consequences.

1.3.3   Large-Scale Vibrations

About 100 earthquakes occur each year with the strength to cause significant damage. The earth's crust (outer layer) surrounds its hot liquid inner core and is broken up into giant plates of rock. Sometimes two plates collide along a fault and pressure builds up until the plates snap into a new position. The release of this traction (pressure) causes vibrations that we feel as an earthquake. When the vibration of the earth has the same frequency as the natural frequency of a building, a resonance occurs and the building vibrations may become very destructive. The Mexico City earthquake of 1985 was especially destructive for buildings 10–14 stories tall since they had natural frequencies near the ground shake frequency. The Northridge, California, earthquake of 1994 registered 6.7 on the Richter scale and yielded motions up to 0.35 m. Typical earthquake frequencies range from 0.2 to 5.0 Hz.

The field of helioseismology has discovered that the sun, being a deformable ball of hot gas, vibrates in millions of resonant modes with the major ones ringing at frequencies between 1 and 5 milli-hz. These modes may ring for days or even months before decaying away. Similar phenomena have been observed by astronomers noting the brightness of other very distant stars. The radial vibration velocity observed in one case was in the 1–3 km/s range.

Our universe is filled with vibrating objects: some big–some small, some near–some far, some good–some bad, shaking an atom and shaking a star! Feel like vibrating? Place your fingertips on your throat and say a long "e" with a big cavity and with a small cavity-shaped throat. Feel the vibes! *This level of vibration would be considered as severe if it was measured on the bearing housings of a large industrial turbine or compressor.*

1.4   HARMFUL EFFECTS OF VIBRATION

Some beneficial reasons to create vibrations include:

(a) Music

(b) Radar/sonar/radio/microwaves

(c) Back massagers

(d) Lithotripsy (for kidney stone fragmentation)

(e) Industrial vibrators for clearing blockages and hang-ups of grain screenings, soya meal, gypsum coal, refined ore, and other materials in bins, chutes, hoppers, and silos

These are the good vibrations. In contrast, most vibrations are adverse to human, machinery, and structural health, and an important engineering objective is to reduce them to harmless levels.

1.4.1   Human Exposure Limits

Body vibration is usually classified according to "whole body vibration" (WBV) or "local vibration" (Griffin, 1990). The three principal possibilities for WBV are sitting on a vibrating seat, standing on a vibrating floor, or lying on a vibrating surface. Local vibration results when a limb or the head contacts a vibrating surface. Effects of vibration on the body depend on frequency, amplitude, and duration and range from "motion sickness" (low frequency–high amplitude) to fatigue-decreased proficiency and permanent damage to hands and arms (high frequency–low amplitude).

The International Standard Organization's (ISO) Standard ISO 2631-1, 1997 "Mechanical Vibration and Shock—Evaluation of Human Exposure to Whole Body Vibration" provides a quantitative, measurable means to determine how severe a particular vibration may be on human health, based on statistical surveys. This document should be directly consulted in an actual design study; however, some general guidelines are that WBV acceleration vibrations less than 0.75 m/s^2 may be mildly disagreeable, from 0.75 to 1.5 m/s^2 may be disagreeable, and higher levels may be very disagreeable. The Standard parses these general divisions into much more finely divided levels and is a "living document" that is periodically updated. Continuous exposure to vibration over some duration of time may be risky to health as illustrated by the ISO standards.

A measure of vibration exposure that includes both amplitude and duration is the vibration dose value (VDV). This is defined as (Griffin, 1990)

$$\text{VDV} = \left[\int_{t=0}^{T} a^4(t)\, dt \right]^{1/4} \tag{1.4.1}$$

where $a(t)$ is the vibration acceleration in m/s^2. The caution zone is reached when the VDV is 8.5 m/s$^{1.75}$ and a health risk occurs for VDV greater than 17 m/s$^{1.75}$. Referring to British standard 6472, Guide to evaluation of human exposure to vibration in buildings, Hassan (2009) provides VDV levels for the threshold of "adverse comment" of people working in various types of buildings and offices. These values range from 0.1 m/s$^{1.75}$ for residential buildings at night to 0.8 m/s$^{1.75}$ for busy offices or workshops.

The transportation safety department of the Australian Transport Safety Bureau identified potential WBV-related health problems as:

(a) Discomfort and interference with activities

(b) Disorders of the joints and muscles and especially the spine

(c) Cardiovascular, respiratory, endocrine, and metabolic changes

(d) Problems in the digestive system

(e) Reproductive damage in females

(f) Impairment of vision or balance

(g) Low back pain arising from early degeneration of the lumbar system

(h) Muscular fatigue and stiffness

The motions referred to thus far represent input motions to the whole body. The vibrations of certain parts of the body could be much worse if internal resonance occurs. Griffin (1990) states that a human body should only be considered to act rigidly for frequencies less than 2 Hz. For instance, the eye's natural frequency (f_n) falls in the range 20–70 Hz, the head relative to shoulders f_n lies between 20 and 30 Hz, and the trunk's f_n lies between 4 and 6 Hz.

Local body vibration may also cause serious health problems. An example of this is vibration that is localized to the hand and arm. Prolonged exposure may result in the hand–arm vibration syndrome (HAVS), which is also known as "white finger," "dead finger," or "Raynaud's syndrome" (Griffin, 1990). HAVS is a vascular (blood vessel) disorder-related disease of increased risk with exposure to cold, loud noise, and tobacco smoke (CDC, 1994). Early signs of HAVS include:

- Tingling fingertips
- Fingertips turning white or blue
- Trouble picking up small objects
- Numbness
- Clumsiness with hands
- Trouble buttoning and zipping clothes
- Reduced sense of heat, cold, and pain in hands

According to the US National Institute of Occupational Safety and Health (NIOSH, 1989), HAVS reduces blood circulation due to narrowing of the blood vessels. This results in one or more fingers becoming white and cold. This condition may become irreversible with long-term vibration exposure. The disease is prevalent among workers using chipping hammers, drills, riveters, grinding wheels, chain saws, and driving motorcycles. Relevant information on HAVS exposure limits may be found in ISO Standards 5349 and 8662 and ANSI S3.34-1986 (American National Standard) as well as in Griffin (1990). Thus, for example, these references indicate that a vibration acceleration level of 30 m/s^2 ($\approx 3g'$s) is generally safe for 1 hour exposure but it may be unsafe for 2 hours or more of exposure. The actual standards should be referenced in any industrial design study. Appropriate use of the standards requires measurement of the acceleration component directed into the hand so as to generate compression rather than shear motion. The standard should be applied to the worst frequency component of the acceleration signal's Fourier series (spectrum). There is also a probabilistic aspect to interpreting the standards. This is illustrated by noting, for instance, that for the 4–8-hour exposure zone, a latency period of 10–20 years is expected to yield vascular symptoms in 10% of the exposed population. The harmful effects of long-term exposure to hand and arm vibration extend beyond blood circulation (vascular) disorders to include a large number of bone and joint disorders (Griffin, 1990).

Figure 1.4.1 Simple cantilever pipe subjected to bending, axial, and torsional loads

1.4.2　High-Cycle Fatigue Failure

The intent here is to present a primer on high-cycle fatigue (HCF) to illustrate the practical importance of studying vibrations. More advanced texts such as Nicholas (2006) or Lee et al. (2012) should be referenced for a more in-depth understanding and for applications. Stress is a measure of the internal or surface force density in an object. For example, the beam shown in Figure 1.4.1 has a cantilever support and a circular cross section and is subjected to a transverse force $F(t)$, axial force $P(t)$, and twisting torque $\tau(t)$. The vibrations caused by these excitations create an internal shear force $V(x, t)$, internal bending moment $M(x, t)$, internal axial force $f(x, t)$, and internal torque $\Gamma(x, t)$ at position x. These internal actions create stresses in beams described by the strength of materials type formulas

$$\sigma_{\text{bend}}(t) = \frac{M(t)c}{I}, \quad \sigma_{\text{axial}}(t) = \frac{P(t)}{A}, \quad \tau_{\text{shear}}(t) = \frac{V(t)}{A}, \quad \tau_{\text{tors}}(t) = \frac{\Gamma(t)c}{J} \qquad (1.4.2)$$

where A is the cross-sectional area, I is the bending area moment of inertia, and J is the torsion constant. As implied by (1.4.2), loads and resulting stresses generally vary with time.

Materials are compared and characterized by the amount of stress they can withstand before breaking. For example, the ultimate strength (stress) for high-strength 340 Aermet steel is $\sigma_{\text{ut}} \approx 325\,000\,\text{lb/in.}^2$, where the more common A36 steel has an ultimate strength $\sigma_{\text{ut}} \approx 56\,000\,\text{lb/in.}^2$. Guess which costs more, or which is more likely to be found in a high-performance aircraft, given that they both have the same density? The amount of stress that a component can tolerate is reduced if the stress varies cyclically with time. This important fact gave birth to the entire subject of fatigue. To demonstrate this, bend an ordinary metal coat hanger by 180°, and you'll find it does not break. However, if the bending deformation is repeated many times, failure will occur, even for angles that are much less than 180°. This phenomenon is referred to as low-cycle fatigue failure if the bent section breaks in less than approximately 1000 cycles and the maximum stress is near the tensile (ultimate) strength S_{ut}. HCF represents the same phenomena of cyclic stress; however, failures occur after 10^3, 10^4, 10^5, 10^6 or higher cycles and the failure stress may be much less than S_{ut} or even much less than the yield stress.

How does this relate to vibrations? Well, within the limits of linear theory, stresses are proportional to strains, which are in turn proportional to displacements, aka vibration. Thus, the larger the vibration deformation becomes, the larger the stress. HCF failures may occur when vibrations become excessive as will be the case if the component has low damping and is being forced at a frequency near to one of its free vibration (natural) frequencies, that is, near resonance.

Several practical examples from industry will illustrate the importance of HCF considerations. Gas turbine engines mix compressed air with fuel, combust the mixture, and expel
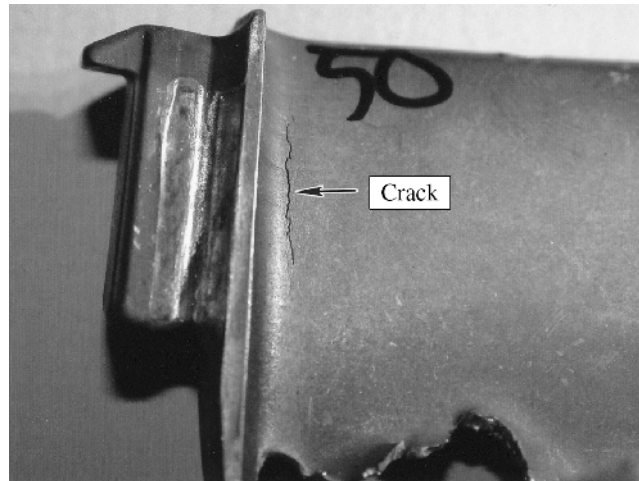
Figure 1.4.2 Turbine blade with high-cycle fatigue crack. Reproduced with permission from Transport Safety Board of Canada

the resulting hot gases through a turbine wheel. The torque that this causes on the turbine wheel may spin a compressor creating compressed air or a generator creating electricity. The air that flows through the compressor is directed by stationary (nonrotating) stator vanes to optimally impinge on the rotating blades. A similar situation occurs with the hot gases in the turbine. Any rotating blade experiences an impulse-type force as it collides with the flow through the passage between two stator vanes. The rotor blade is then excited at the frequency

$$f_{\text{excit}} = (\text{Rotor spin frequency}) * (\text{Number of stator vanes}) \qquad (1.4.3)$$

which is referred to as the blade-pass frequency. This excitation causes the blades to vibrate causing time-varying (alternating) stresses along with the static, centrifugal-induced stress in the blades. The level of alternating stress that is tolerable is reduced by the presence of the static (mean), tensile, and centrifugal stresses. Figure 1.4.2 shows an HCF crack on a blade from an aircraft gas turbine engine.

The combination of *alternating stress and mean stress* may cause an HCF failure (catastrophic crack) if the rotor blade is not properly designed. The vibration (and stress) level will substantially increase if f_{excit} or one of its harmonics is in the vicinity of a rotor blade natural frequency, that is, a resonant condition. HCF of blades is a constant concern of all turbine and compressor designers with applications to steam or gas turbines for power generation, aircraft, helicopters, ships, chemical processing, or even to the space shuttle main engines. The consequences of "throwing off" a cracked blade are frequently catastrophic and sometimes fatal. The US Air Force has determined that more than 50% of accidents involving aircraft damage result from HCF.

Piping and tubing systems are also subjected to vibration-induced cyclic stress due to pressure pulsation forces generated by attached machinery, such as reciprocating compressors, or from internally generated vortices. These systems are also subjected to static stress from internal pressure and partially constrained thermal expansion. Experienced chemical plant personnel know that an HCF-induced crack in a high-pressure gas line will sometimes emit a high-pitch whistle as the gas escapes through the crack, signaling all nearby workers to shut down the machinery and flee.
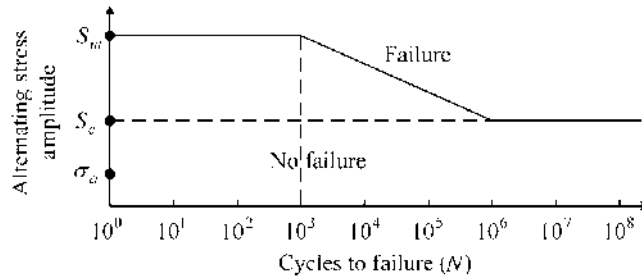
Figure 1.4.3 Simplified S–N curve for HCF failure evaluation plotted on log–log format

These examples illustrate cases where vibration of machinery and structures induces cyclic stress, which may cause HCF failure. This may occur at stress levels well below the yield stress or ultimate/tensile strength (S_{ut}), which is illustrated by the simplified *S–N (alternating stress amplitude vs. number of cycles to cause failure) diagram* in Figure 1.4.3. The sloped portion of the curve is of primary interest and has the general form

$$S_{\text{failure}} = \gamma N^{\alpha} \tag{1.4.4}$$

where the constants γ and α are determined experimentally and are a property of the material.

The *endurance limit* stress S_e is defined as the level below which failure will not occur independent of the number of cycles. The value of S_e is most accurately obtained by experiment with the material and geometry of interest; however, it is sometimes approximated for steels as (Shigley, 1989)

$$S'_e = \begin{cases} 0.50 * S_{ut}, & S_{ut} \leq 1400\,\text{MPa} \ (200\,\text{kpsi}) \\ 700\,\text{MPa}, & S_{ut} > 1400\,\text{MPa} \\ 100\,\text{kpsi}, & S_{ut} > 200\,\text{kpsi} \end{cases} \tag{1.4.5}$$
$$S_e = kS'_e$$

where k is a series product of modifying factors and S'_e is the endurance stress limit of a highly polished, cylindrical specimen at room temperature. The modifying *(Marin) factors* account for surface condition, size, load types, temperature, plating, corrosion, and so on. In addition, a modifying factor also may be applied to account for the reliability of S'_e, which is a statistical quantity, typically provided in tables as a mean value over many tests of "identical" specimens. This modifying factor is usually based on the assumption of a Gaussian distribution for the measured endurance limit and a ratio of its standard deviation to the mean value of, for instance, 8%. The maximum value of stress taken over the entire component should be utilized in Figure 1.4.3 since stress varies spatially.

Figure 1.4.4 shows a weight attached to the end of a cantilevered beam. The static weight causes a static deflection and strain, which causes a constant mean stress σ_m that is maximum at the wall since the moment is largest there and the nominal beam stress is magnified by the local geometry (stress concentration) at the connection to the wall. The weight vibrates about its statically deflected position creating a time-varying deflection and corresponding alternating stress.
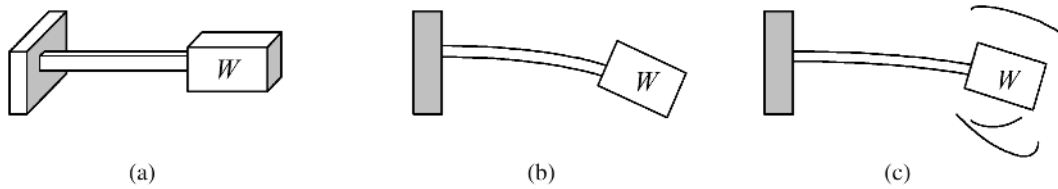
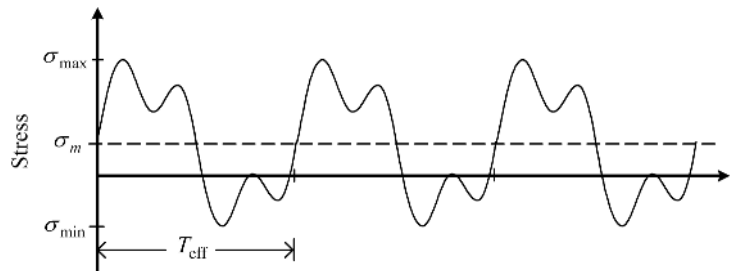**Figure 1.4.4** (a) Cantilevered block with (b) static (mean) and (c) static plus dynamic deflections and stresses

Figure 1.4.5 Stress response with multiple frequencies and a static component
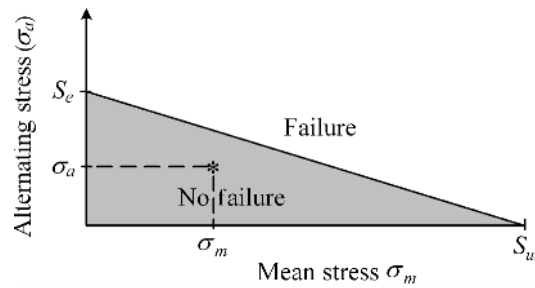

**Figure 1.4.6** Modified Goodman diagram for combined static and dynamic stresses

Stress waveforms may contain components at several frequencies including a static component as illustrated in Figure 1.4.5. Define the alternating stress amplitude as

$$\sigma_a = \frac{\sigma_{max} - \sigma_{min}}{2} \qquad (1.4.6)$$

Then σ_a can be utilized in Figure 1.4.3 to estimate the life of the component. Collins (1981) states that the minor "frequency component" (small bumps) in Figure 1.4.5 may be ignored if they are substantially smaller than the primary component. The effective cycle period becomes T_{eff} as shown in Figure 1.4.5. The effect of the "static" or "mean" stress in Figure 1.4.5

$$\sigma_m = \frac{\sigma_{max} + \sigma_{min}}{2} \qquad (1.4.7)$$

is to reduce the alternating stress level below which HCF failure will not occur, that is, reduce the infinite life stress threshold to a value less than S_e. This is illustrated by the modified *Goodman diagram* in Figure 1.4.6. The failure line connecting S_e and S_{ut} provides the effective endurance limit $S_{e,eff}$ as a function of the mean stress σ_m.
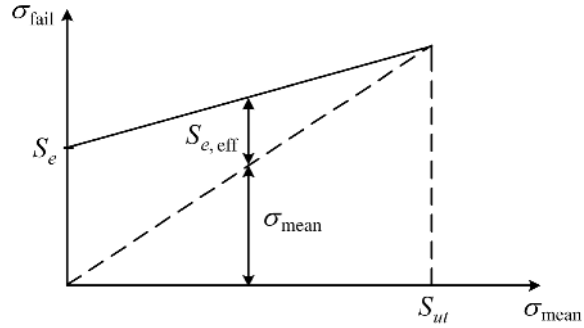
Figure 1.4.7 Peak stress at failure versus mean tensile stress

This figure is only applicable for positive values of σ_m (tensile stress). For compressive σ_m values, the part will eventually fail if $\sigma_a > S_e$ or will fail if $\sigma_m > S_{ut}$, that is, the static and dynamic failure criteria are uncoupled. The obvious implication of the Goodman diagram is that the effective endurance limit $S_{e,eff}$ decreases as mean stress increases. Another view is that the alternating stress amplitude should be divided by this same reduction factor when using the S–N curve in Figure 1.4.3, that is, utilize the following effective alternating stress in Figure 1.4.3:

$$\sigma_{a,eff} = \frac{\sigma_a}{1 - \sigma_m/S_{ut}} \tag{1.4.8}$$

Although the endurance limit may decrease with increasing tensile mean stress, the maximum total stress (mean plus alternating) for which failure will eventually occur typically increases with mean stress as indicated by Figure 1.4.7.

Fatigue test data is generally consistent with Figure 1.4.7. Fatigue data is available from several sources and is generally presented in the form depicted in Figure 1.4.8. This figure is "Figure 2.3.1.3.8(l). Best-fit S–N curves for notched, $K_T = 3.3$, AISI 4340 alloy steel bar, $F_{TU} = 200$ ksi, longitudinal direction" in the extensive database supported by MMPDS-08, Battelle Memorial Institute, at www.mmpds.org. The "stress ratio" R is defined by

$$R = \frac{\sigma_{min}}{\sigma_{max}} = \frac{\sigma_m - \sigma_a}{\sigma_m + \sigma_a} = \frac{1 - \sigma_a/\sigma_m}{1 + \sigma_a/\sigma_m} \tag{1.4.9}$$

which increases monotonically as σ_a/σ_m decreases. Note that $R = -1$ corresponds to a zero mean stress, $\sigma_m = 0$, condition, that is, the maximum stress is the amplitude of the alternating stress. Similarly, $R = 1$ corresponds to a zero alternating stress, $\sigma_a = 0$, condition, that is, the maximum stress is the mean stress. The test data is typically accompanied by curve fits in forms similar to

$$\text{Cycles to failure} = 10^{\{a_1 - a_2 * \log_{10}[\sigma_{max} * (1 - R)^{a_3} - a_4]\}} \tag{1.4.10}$$

where σ_{max} is in units of ksi and the a_i are constants. Care must be taken to utilize the curve fit equation only when the argument $[\sigma_{max} * (1 - R)^{a_3} - a_4]$ of the logarithm is positive.

Note that the peak allowable stress increases as R increases, indicating an increase in total allowable stress as σ_a/σ_m decreases. Some components experience a nearly pure state of torsional shear stress such as a shaft in an industrial machinery train. The shear stress in a circular shaft or coupling due to pure torsional torque loading is given by

$$\tau = \frac{T r_{outer}}{J} \text{ where } J = \frac{\pi}{2} \left(r_{outer}^4 - r_{inner}^4 \right) \tag{1.4.11}$$
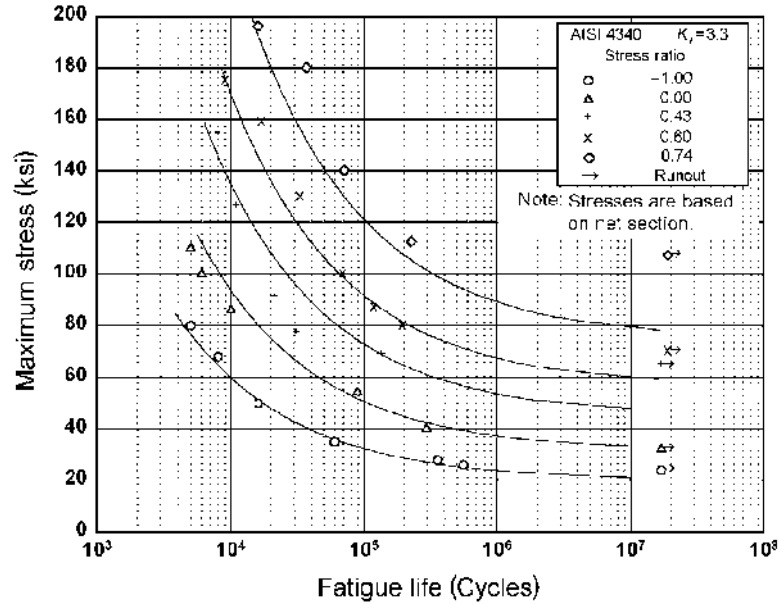
Figure 1.4.8 Typical S–N curves for various R values MMPDS-08. (Figure 2.3.1.3.8(I). Best-fit S–N curves for notched, $K_T = 3.3$, AISI 4340 alloy steel bar, $F_{TU} = 200$ ksi, longitudinal direction.) Reproduced with permission of Battelle Memorial Institute

Figure 1.4.9 Plot of effective torsional stress endurance limit (solid line) versus mean torsional shear stress
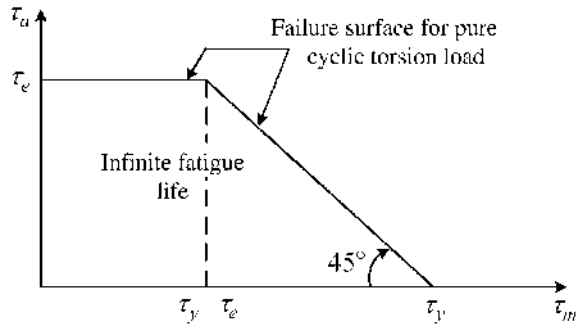
where τ is the shear stress, T is the transmitted torque through the coupling/shaft, r_{outer} is the outer radius of the coupling/shaft, r_{inner} is the inner radius of the coupling/shaft, and J is the torsion constant. For this case, Wang (2006) states that "Experimental results tend to show that the value of the mean shear stress has no influence on the fatigue life of a ductile structural component subjected to cyclic torsional loading as long as the maximum stress is less than the yield strength of the material. Hence, the plot of the alternating shear stress τ_a versus mean shear stress τ_m is bound by a horizontal line with $\tau_a = \tau_e$ and a 45 deg yield line." This is illustrated in Figure 1.4.9.

The parameters in Figure 1.4.9 are τ_e, the torsional endurance limit; τ_y, the torsional yield strength; τ_m, the torsional mean stress; and τ_a, the torsional alternating stress. The material will fail after a finite number of stress cycles if either

if

$$\tau_m < \tau_y - \tau_e \text{ and } \tau_a > \tau_e \tag{1.4.12}$$

then $\tau_{a,eff} = \tau_a$ (*mean stress has no influence*)

or if

$$\tau_m > \tau_y - \tau_e \text{ and } \tau_a > \tau_y - \tau_m \tag{1.4.13}$$

then $\tau_{a,eff} = \tau_a \dfrac{\tau_e}{\tau_y - \tau_m}$ (*mean stress has influence*).

Most components of structural systems are subjected in general to complex states of combined normal and shear stresses. The above approach for evaluating HCF failure may still be utilized by employing the equivalent, or "von Mises (VM)", stress utilized in the von Mises–Hencky, or distortion energy yielding failure theory. This failure theory states that the material will yield if the actual structure's local, distortion-strain energy density, due solely to distortion and not to the hydrostatic stress components, exceeds the distortion-strain energy density in a uniaxially loaded test specimen, at the yield condition. This condition produces the following condition for yield failure

$$\sigma' \geq \frac{S_Y}{n} \tag{1.4.14}$$

where S_Y is the yield strength of the material (in general another statistical quantity), n is the selected design safety factor, and σ' is the so-called von Mises, or equivalent, stress

$$
\begin{aligned}
\sigma' &= \frac{1}{\sqrt{2}} \sqrt{(\sigma_1 - \sigma_2)^2 + (\sigma_2 - \sigma_3)^2 + (\sigma_3 - \sigma_1)^2} \\
&= \frac{1}{\sqrt{2}} \sqrt{(\sigma_X - \sigma_Y)^2 + (\sigma_Y - \sigma_Z)^2 + (\sigma_Z - \sigma_X)^2 + 6(\tau_{XY}^2 + \tau_{YZ}^2 + \tau_{XZ}^2)}
\end{aligned}
\tag{1.4.15}
$$

where $(1, 2, 3)$ indicates principal normal stresses and (X, Y, Z) indicates Cartesian coordinate, component stresses. The alternating amplitude and mean value for each component or principal stress in (1.4.15) are evaluated by applying equations (1.4.6) and (1.4.7) to the respective stress's time history. These alternating and mean values are then utilized to determine the *equivalent mean VM stress* and the *equivalent alternating VM stress* as follows:

$$^m\sigma' = \frac{1}{\sqrt{2}} \sqrt{\left(^m\sigma_X - {}^m\sigma_Y\right)^2 + \left(^m\sigma_Y - {}^m\sigma_Z\right)^2 + \left(^m\sigma_Z - {}^m\sigma_X\right)^2 + 6\left(^m\tau_{XY}^2 + {}^m\tau_{YZ}^2 + {}^m\tau_{XZ}^2\right)}$$

$$\tag{1.4.16}$$

$$^a\sigma' = \frac{1}{\sqrt{2}} \sqrt{\left(^a\sigma_X - {}^a\sigma_Y\right)^2 + \left(^a\sigma_Y - {}^a\sigma_Z\right)^2 + \left(^a\sigma_Z - {}^a\sigma_X\right)^2 + 6\left(^a\tau_{XY}^2 + {}^a\tau_{YZ}^2 + {}^a\tau_{XZ}^2\right)} \tag{1.4.17}$$

Then $^m\sigma'$ and $^a\sigma'$ are employed in Figure 1.4.6, in place of σ_m and σ_a, respectively, to determine whether HCF failure will occur, including the effects of the corresponding safety factor and the reduced value of the endurance limit due to the mean stress $^m\sigma'$. Vibration simulation models are frequently assembled from beam, plate, bar, or other structural modeling components that provide nominal stress values. Consideration of abrupt changes in geometry such as holes, fillets, welds, and so on requires multiplication of the nominal stresses by respective *stress concentration factors* to obtain accurate stress values (Budynas and

Nisbett, 2008). The equivalent stresses in (1.4.16) and (1.4.17) then assume the more complicated forms

$$
{}^{\mathrm{m}}\sigma' = \frac{1}{\sqrt{2}} \sqrt{\begin{array}{l} \left({}^{\mathrm{m}}\sigma_X K_X - {}^{\mathrm{m}}\sigma_Y K_Y\right)^2 + \left({}^{\mathrm{m}}\sigma_Y K_Y - {}^{\mathrm{m}}\sigma_Z K_Z\right)^2 + \left({}^{\mathrm{m}}\sigma_Z K_Z - {}^{\mathrm{m}}\sigma_X K_X\right)^2 \\ + 6\left[\left({}^{\mathrm{m}}\tau_{XY} K_{XY}\right)^2 + \left({}^{\mathrm{m}}\tau_{YZ} K_{YZ}\right)^2 + \left({}^{\mathrm{m}}\tau_{XZ} K_{XZ}\right)^2\right] \end{array}} \tag{1.4.18}
$$

$$
{}^{\mathrm{a}}\sigma' = \frac{1}{\sqrt{2}} \sqrt{\begin{array}{l} \left({}^{\mathrm{a}}\sigma_X K_X - {}^{\mathrm{a}}\sigma_Y K_Y\right)^2 + \left({}^{\mathrm{a}}\sigma_Y K_Y - {}^{\mathrm{a}}\sigma_Z K_Z\right)^2 + \left({}^{\mathrm{a}}\sigma_Z K_Z - {}^{\mathrm{a}}\sigma_X K_X\right)^2 \\ + 6\left[\left({}^{\mathrm{a}}\tau_{XY} K_{XY}\right)^2 + \left({}^{\mathrm{a}}\tau_{YZ} K_{YZ}\right)^2 + \left({}^{\mathrm{a}}\tau_{XZ} K_{XZ}\right)^2\right] \end{array}} \tag{1.4.19}
$$

where the K terms are stress concentration factors derived from test data or analysis (Pilkey, 1997). The K factors can also be modified from their static load values for application to fatigue problems as indicated in Budynas and Nisbett (2008).

1.4.2.1   Miner–Palmgren Rule

Suppose an object is exposed to N_{loads} distinct sets of loadings characterized by effective alternating stress amplitudes $\sigma_{\mathrm{a}i}$, actual number of load cycles n_i at this stress amplitude, and number of load cycles N_i for failure at this stress amplitude. Define the damage done by the ith load set as

$$
R_i = \frac{n_i}{N_i} \tag{1.4.20}
$$

Then the object is predicted to fail by the *Miner–Palmgren rule* when the damage

$$
D = \sum_{i=1}^{N_{\mathrm{loads}}} R_i = \beta \tag{1.4.21}
$$

where typically $\beta = 1$; however, for a more conservative approach, some researchers utilize 0.6 or 0.7 instead. Stress will be calculated at many locations in the component's model, and the part will be predicted to fail if any of these locations have a cumulative fatigue damage that exceeds β. A thorough fatigue analysis requires that the damage be evaluated at many locations.

1.4.2.2   Rainflow Cycle Counting

In general, loading may be nonperiodic (Chapter 6) but recurring and cause vibratory deflections and stresses. The most common example is random excitation as might occur on a wind turbine blade or offshore platform. Another occurrence is a system subjected to a transient load that causes vibratory stresses and is applied at well-separated and varying time intervals, such as the transient start-up torque applied by an electric motor to a machinery train. It is not obvious how one should properly identify load cycles and equivalent alternating stress amplitudes to utilize (1.4.20), (1.4.21), and Figure 1.4.2 to predict damage and life for this type of loading. The "rainflow method" is the most common of the "cycle counting" techniques that provide a systematic means to identify arrays of alternating stress amplitudes and corresponding mean stresses during an arbitrary varying stress time history.
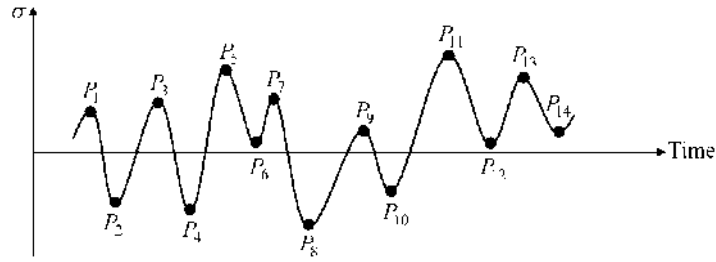
Figure 1.4.10 Stress extrema set in a stress versus time history

Consider the following definitions:

Extremum: a point P_i in a stress versus time history when the stress is either a local maximum or minimum. The plural of extremum is extrema. Reference Figure 1.4.10.

Extrema set: collection of extremum points in a stress versus time history.

Extrema pair: two members in an extrema set.

Extrema trio: three consecutive members (a, b, c) in an extrema set.

Begin point: first point in an extrema set.

Change C: absolute value of the difference between two stresses in an extrema pair.

Mean stress: average of the two stresses in an extrema pair.

Alternating stress: one-half of the absolute difference of the two stresses in an extrema pair.

The overarching logic of the method is to systematically locate extrema trios (a, b, c) such that the change C_{bc} between (b, c) is greater than the change C_{ab} between (a, b). This justifies counting C_{bc} as ½ load cycle. The rainflow procedure is illustrated by the example given below. Start with the extrema set that contains all extrema in a stress versus time history, for example, P_1 through P_{14} in Figure 1.4.10. These extrema and their values (in ksi) are given in row 1 of Table 1.4.1. Table 1.4.1 lists the 14 steps needed to identify the equivalent load cycles for given stress time history. The extrema set of step i is given by the numbers in row i of Table 1.4.1. The number of members in the extrema set diminishes as the rainflow process proceeds. Each step considers a new trio (a, b, c) of points in the current extrema set and compares the respective changes C_{ab} and C_{bc} of extrema pairs (a, b) and (b, c). The trio (a, b, c) are boldened for each step in Table 1.4.1.

As demonstrated in Table 1.4.2 for each rainflow step:

- Trio (a, b, c) are *always* three consecutive points in the updated extrema set.
- The trio (a, b, c) is updated in going from step i to step $i + 1$ in the following manner: Point "c" is the next point in the extrema set in going from step i to step $i + 1$, with the exception that if in step i (point "a" is not the begin point of the extrema set and $(C_{bc}/C_{ab}) \geq 1$), then in step $i + 1$ point "a" is set equal to the begin point.
- If $(C_{bc}/C_{ab}) \geq 1$ and the begin point and "a" are the same, then remove point "a" from the extrema set, and accumulate ½ cycle of stress with the mean and alternating stress of extrema pair (a, b).
- If $(C_{bc}/C_{ab}) \geq 1$ and the begin point and "a" are different, then remove points "a" and "b" from the extrema set, and accumulate 1 cycle of stress with the mean and alternating stress of extrema pair (a, b).
- If $(C_{bc}/C_{ab}) < 1$, then no points are removed from the extrema set and no load cycles are accumulated.

Table 1.4.1   Rainflow points for Figure 1.4.10

| Point | 1 | 2 | 3 | 4 | 5 | 6 | 7 | 8 | 9 | 10 | 11 | 12 | 13 | 14 |
step	(8)	(−12)	(14)	(−14)	(18)	(4)	(15)	(−16)	(5)	(−8)	(20)	(3)	(16)	(7)
1	**1**	**2**	**3**	4	5	6	7	8	9	10	11	12	1	14
2	—	**2**	**3**	**4**	5	6	7	8	9	10	11	12	13	14
3	—	—	**3**	**4**	**5**	6	7	8	9	10	11	12	13	14
4	—	—	—	**4**	**5**	**6**	7	8	9	10	11	12	13	14
5	—	—	—	4	**5**	**6**	**7**	8	9	10	11	12	13	14
6	—	—	—	4	5	**6**	**7**	**8**	9	10	11	12	13	14
7	—	—	—	**4**	**5**	—	—	**8**	9	10	11	12	13	14
8	—	—	—	—	**5**	—	—	**8**	**9**	10	11	12	13	14
9	—	—	—	—	5	—	—	**8**	**9**	**10**	11	12	13	14
10	—	—	—	—	5	—	—	8	**9**	**10**	**11**	12	13	14
11	—	—	—	—	**5**	—	—	**8**	—	—	**11**	12	13	14
12	—	—	—	—	—	—	—	**8**	—	—	**11**	**12**	13	14
13	—	—	—	—	—	—	—	8	—	—	**11**	**12**	**13**	14
14	—	—	—	—	—	—	—	8	—	—	11	**12**	**13**	**14**

Parentheses: stress value in *ksi*.
Bold indicates "*a*," "*b*," and "*c*" points of current step.

Table 1.4.2   Rainflow cycle counts for Figure 1.4.10

Step	Begin point	a	b	c	C_{ab}	C_{bc}	Removed[a] point "a" or "a" and "b"	Number of cycles of (a,b)[a]	σ_{min}[b]	σ_{max}[b]	σ_m[b]	σ_a[b]
1	1	1	2	3	20	26	1	½	−12	8	−2	10
2	2	2	3	4	26	28	2	½	−12	14	1	13
3	3	3	4	5	28	32	3	½	−14	14	0	14
4	4	4	5	6	32	22	—	—	—	—	—	—
5	4	5	6	7	14	11	—	—	—	—	—	—
6	4	6	7	8	11	31	6 and 7	1	4	15	9.5	5.5
7	4	4	5	8	32	34	4	½	−14	18	2	16
8	5	5	8	9	34	21	—	—	—	—	—	—
9	5	8	9	10	21	13	—	—	—	—	—	—
10	5	9	10	11	13	28	9 and 10	1	−8	5	−1.5	6.5
11	5	5	8	11	34	36	5	½	−16	18	1	17
12	8	8	11	12	36	17	—	—	—	—	—	—
13	8	11	12	13	17	13	—	—	—	—	—	—
14	8	12	13	14	13	9	—	—	—	—	—	—
15	8	8	11	—	36	—	8	½	−16	20	2	18
16	11	11	12	—	17	—	11	½	3	20	11.5	8.5
17	12	12	13	—	13	—	12	½	3	16	9.5	6.5
18	13	13	14	—	9	—	13	½	7	16	11.5	4.5

[a] Only if $C_{bc} > C_{ab}$.
[b] Values for extrema pair interval (a, b).

Table 1.4.3   Load cycles for example in Table 1.4.1

j	1	2	3	4	5	6	7	8	9	10	11
No. of cycles n_i	½	½	½	1	½	1	½	½	½	½	½
σ_m (ksi)	−2	1	0	9.5	2	−1.5	1	2	11.5	9.5	11.5
σ_a (ksi)	10	13	14	5.5	16	6.5	17	18	8.5	6.5	4.5
$\sigma_{a,eff}$ (ksi)	10	13.5	14	8.9	17.4	6.5	17.7	19.6	15.7	10.5	8.3
$N_i \times 10^5$	0.33	0.07	0.06	0.60	0.02	2.82	0.019	0.011	0.034	0.259	0.815

The above procedure is repeated until point "c" of the trio (a, b, c) is the last extrema point. A ½ load cycle is counted for each of the surviving consecutive extrema pairs in the final extrema set. This is illustrated by steps 15–18 in Table 1.4.2.

For the sake of illustration, assume that $S_e = 5\,\text{ksi}$, $S_{ut} = 25\,\text{ksi}$ and the S–N curve follows the following common form (Budynas and Nisbett, 2008):

$$\gamma = \frac{(\phi S_{ut})^2}{S_e} = 80000, \quad \alpha = -\frac{1}{3}\log_{10}\left(\frac{\phi S_{ut}}{S_e}\right) = -0.200$$

$$\text{Cycles to failure} = N = \begin{cases} \left(\dfrac{\sigma_{a,eff}}{\gamma}\right)^{1/\alpha} & \text{if } \sigma_{a,eff} > S_e \\ \infty & \text{if } \sigma_{a,eff} < S_e \end{cases}$$

where ϕ is a constant that is taken as 0.8 for this example. The effective alternating stress is obtained from the modified Goodman formula (1.4.8) as

$$\sigma_{a,eff} = \begin{cases} \dfrac{\sigma_a}{1 - (\sigma_m / S_{ut})} & \text{if } \sigma_m > 0 \\ \sigma_a & \text{if } \sigma_m \leq 0 \end{cases}$$

Table 1.4.3 summarizes the load cycles obtained by the rainflow method in Table 1.4.2, the corresponding effective alternating stresses, and the cycles to failure.

The damage as given by (1.4.21) is

$$D = \sum_{i=1}^{11} \frac{n_i}{N_i} = .0013$$

This implies that for a $D = 1$ failure criteria, $1/D = 765$ repetitions of the sample load set would be required to fail the component.

The rainflow counting algorithm is tedious by hand for a large data set and is frequently implemented in an automated form such as found in the MATLAB code (Nieslony, 2010). Additional reading on the rainflow method may be found in ASTM E-1049–85 (2011).

1.4.3   Rotating Machinery Vibration

Spinning shafts of industrial, aviation, and aerospace machinery such as turbines, compressors, motors, fans, and so on vibrate due to their inherent imbalance, misalignment, looseness, resonance, inadequate damping, interaction with the transmitted liquid or gas, gear

forces, failed bearings, and so on. Most of the machines mentioned above operate at high speeds (1000–50 000 rpm) and have very small clearances between the spinning (rotor) and stationary (stator) components. These clearances may be as small as 0.01 mm per 1 cm of shaft diameter. This accentuates the potential seriousness of controlling vibration, which may lead to internal rubs followed by loss of machinery, product, and, in rare instances, lives. For this reason, standards have been established to aid in purchasing and operating various types of rotating machine. The American Petroleum Institute (API) *standards* are often utilized throughout the petrochemical and process industries. Some API standards include:

- API STD 610—Centrifugal Pumps for General Refinery Service
- API STD 611—General Purpose Steam Turbines for Petroleum, Chemical, and Gas Industry Services
- API STD 617—Axial and Centrifugal Compressors and Expander—Compressors for Petroleum, Chemical, and Gas Industry Services
- API Standard Paragraphs Rotordynamic Tutorial: Lateral Critical Speeds, Unbalance Response, Stability, Train Torsionals, and Rotor Balancing. API Recommended Practice 684, 2nd Ed., August 2005, Reaffirmed, November 2010

An example rule from API STD 617 is as follows: Let x represent the peak-to-peak vibration of the rotating shaft relative to the stator at the bearing locations, and then the maximum allowable value for x is

$$x \leq 25 * \sqrt{\frac{12\,000}{N_{\max}}}(\mu m, \text{p-p}) \qquad (1.4.22)$$

where $N_{\max}$ is the maximum continuous speed of the compressor in revolutions per minute. It is very important to note that the API standards are "living documents" that are being continuously updated by panels of experts and that the standards should be consulted directly for use of the most up-to-date formulas for actual industrial applications.

Recall the phenomenon of resonance that was discussed in Sections **1.2** (Tacoma Narrows Bridge), **1.3** (clocks and earthquakes), and **1.4** (human body). Machinery resonance is a particularly detrimental problem, which may lead to premature and possibly catastrophic failure. Resonance occurs when an excitation (forcing) frequency coincides with a natural frequency. An excitation frequency in rotating machinery is the spin (rotational speed) frequency since mass imbalance forces of the rotor vary sinusoidally at the spin frequency. Consequently, the operating speed range of most machinery is kept well separated from any bending natural frequencies of the spinning shaft. API 684 provides rules pertaining to designing and operating rotating machinery in a manner to avoid resonance, which for rotating machinery is referred to as "critical speed." The API standards account for the possible presence of a resonance both above and below the operating speed (rpm) range (OSR) of the machine, by defining a below OSR *minimum separation margin* (SM) and an above OSR minimum SM. As one might expect, the specified minimum SM increases as the intensity (danger) of the resonance increases. Intensity is quantified as the amplification factor AF, which increases as the resonance peak increases in relative height, and is calculated using the half power point method (Eqs. (7.3.52) and (7.3.53), Figure 7.3.9).

A second source for vibration severity guidelines in rotating machinery is the International Organization for Standardization (ISO). The ISO Standard ISO 3945-1977(E) entitled "Mechanical Vibration for Large Rotating Machines with Speed Ranges from 10 to 200 rev/s—Measurement and Evaluation of Vibration Severity in situ" bases vibration

Table 1.4.4   Example vibration severity table—in terms of peak,
RMS vibration velocity

v_{rms} (mm/s)	v_{rms} (in./s)	Condition
<1.27	<0.05	Smooth
>1.27 and <3.8	>0.15 and <0.15	Mild
>3.8 and <10.2	>0.15 and <0.4	Rough
>10.2 and <15.2	>0.4 and <0.6	Severe
>15.2	>0.6	Unacceptable

severity on the measured velocity of vibration *on all bearing housings* of a machine.
Specifically, the rms velocity

$$v_{rms} = \sqrt{\frac{1}{T}\int_0^T v^2(t)\ dt} \tag{1.4.23}$$

is utilized, where T is the total measurement period and $v(t)$ is the measured vibration
velocity in the frequency range 10–1000 Hz. The velocity severity measure v_{rms} may also
be evaluated from the relation (1.2.11)

$$v_{rms} \approx \sqrt{\frac{1}{2}\left(v_1^2 + v_2^2 + \cdots + v_n^2\right)} \tag{1.4.24}$$

if the Fourier frequency component amplitudes $v_1\ \ v_2\ \ \cdots\ \ v_n$ of $v(t)$ are known. Let v_{rms}^{max}
represent the maximum value of v_{rms} over all measurement locations (typically two bearing
housings) and directions (typically horizontal, vertical, and axial) on a machine. Similar
standards are published by other organizations and vibration instrumentation manufacturers.
Table 1.4.4 shows a sample chart presented only for illustration purposes. Actual standards
from ISO or other sources should be consulted in practice.

It is notable that the intent of the standard is to provide an evaluation of machinery
health based upon a relatively easily taken set of measurements and the accumulated expe-
rience of the standard's authors. This approach is clearly justified by the time and cost asso-
ciated with surveying large numbers of rotating machines in chemical, refinery, paper
processing, power, steel, and equipment manufacturing plants and also on ships. A more
detailed set of measurements such as stress, force, and so on should be made if high vibration
is indicated by use of tables in the standards.

Vibration in rotating machinery most often results from mass imbalance of the spinning
shaft. This causes centrifugal forces that deflect the shaft and react against the bearings and
machinery support structure in a sinusoidally varying manner. The corresponding excitation
frequency is the rotational speed frequency of the shaft. ISO has developed standards to
specify acceptable *imbalance* levels since the imbalance force is an important driver (source)
of vibrations. For process equipment such as gas and steam turbines, turbo-compressors,
turbine-driven pumps, and so on, ISO 1940-1973(E) recommends

$$e\omega \le 2.5\,\text{mm}/\text{s} \tag{1.4.25}$$

where

$$\begin{aligned} e = \text{offset of the rotating assembly's mass center} \\ \text{relative to its geometric center (spin axis) in mm} \end{aligned} \tag{1.4.26}$$

$$\omega = \text{spin frequency of the rotating assembly in rad/s} \tag{1.4.27}$$

For example, consider a steam turbine rotor that weighs 1000 N and spins at 10 000 rpm (1047 rad/s). The recommended maximum eccentricity level becomes

$$e = \frac{2.5\,\text{mm/s}}{1047\,\text{rad/s}} = 2.4\,\mu\text{m} \tag{1.4.28}$$

The centrifugal force corresponding to this mass eccentricity and speed is

$$F_c = me\omega^2 = \frac{1000\,\text{N}}{9.8\,\text{m/s}^2} * 2.4 \times 10^{-6}\,\text{m} * \left(1047\,\text{s}^{-1}\right)^2 = 268\,\text{N} \tag{1.4.29}$$

This represents the dynamic force transmitted through the bearings only if the rotational speed frequency is well below all rotating assembly or support natural frequencies. The transmitted force may be much higher at resonance and much lower at shaft speeds well above resonance.

It is important to note that most standards are "living documents" that evolve as the understanding of related anomalous vibrations is increased through experience and research. The latest standards should be referred to in actual practice.

EXAMPLE 1.4.1   *Effective Endurance Limit, Safety Factor, and Vibration Severity*

A large, motor-driven fan is supported at the end of a uniform pipe, which is fastened to a fixed wall. The pipe is modeled as a massless, cantilevered Euler beam (Figure E1.4.1(a)).

The pipe may eventually fail (crack) due to HCF if the alternating component of the von Mises stress $^a\sigma'$ at the wall exceeds the effective endurance limit for the pipe material accounting for the mean von Mises stress $^m\sigma'$. The equation for the boundary curve in the modified Goodman diagram of Figure 1.4.6 provides the effective endurance limit as

$$S_{e,\text{eff}} = S_e - \frac{S_e}{S_{ut}}\left(^m\sigma'\right) \tag{1}$$

The vertical, transverse deflection $\delta_{\text{tip}}^T(t)$ at the tip of the beam has a mean (constant) component δ_m^T due to the weight of the motor/fan assembly and a sinusoidally varying component $\delta_a^T(t)$ due to the rotating imbalance force of the fan

$$\delta^T(t) = \delta_m^T + \delta_a^T(t) = \bar{\delta}_m^T + \bar{\delta}_a^T \sin(\omega t) \tag{2}$$
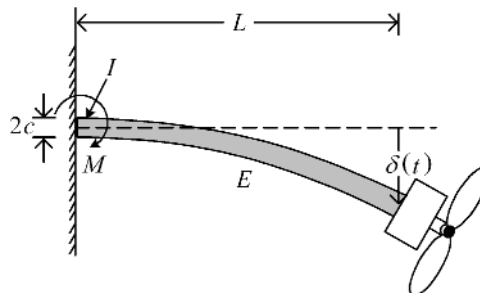
Figure E1.4.1(a) Motor supported by cantilever pipe

The term $\bar{\delta}_a^T \sin(\omega t)$ represents the *vibration*. In addition, the fan blade–air interaction forces cause a static torque Γ_{fan} about the pipe axis and a static, tensile force F_{fan} along the pipe axis. These cause the constant axial and torsional deflections δ_m^A and θ_m^A, respectively, at the tip of the beam.

Let F_{wall}, M_{wall}, and Γ_{wall} be the axial force, bending moment, and torque at the wall, respectively. Then the maximum values of the component, nominal stresses at the wall become

$$\sigma_{\text{axial}} = \frac{F_{\text{wall}}}{A}, \quad \sigma_{\text{bend}} = \frac{M_{\text{wall}} * D_O}{2I}, \quad \tau_{\text{shear}} = \frac{\Gamma_{\text{wall}} * D_O}{2J} \tag{3}$$

where

$$I = \text{bending moment of inertia} = \frac{\pi}{64}\left(D_O^4 - D_I^4\right)$$

$$J = \text{torsion moment of inertia} = \frac{\pi}{32}\left(D_O^4 - D_I^4\right)$$

$$A = \text{pipe cross-sectional area} = \frac{\pi}{4}\left(D_O^2 - D_I^2\right) \tag{4}$$

$$D_O, D_I = \text{outer and inner diameters of the pipe}$$

The load combination described above only produces a normal stress σ_X along the direction of the pipe axis and a shear stress τ_{XY} on the pipe cross section. The corresponding stress concentration factors at the pipe-wall connection plane are K_X and K_{XY}, respectively. All of the remaining stress components are zero. The parameter values for this problem are

$$E = 30.0 \times 10^6\,\text{psi}, \ G = 12.0 \times 10^6\,\text{psi}, \ K_X = 3.0, \ K_{XY} = 2.0, \ L = 40\,\text{in.}, \ D_O = 3.5\,\text{in.}, \ D_I = 3.0\,\text{in.}$$

$$S_{\text{ut}} = 100000\,\text{psi}, \ S_e = 25000\,\text{psi} \ (\text{for a zero mean stress state and includes}$$

$$\text{Marin correction factors})$$

$$\bar{\delta}_m^T = 0.080\,\text{in.}, \ \bar{\delta}_a^T = 0.020\,\text{in.}, \ \delta_m^A = 0.0005\,\text{in.}, \ \theta_m^A = 0.002\,\text{rad}$$

$$\tag{5}$$

where X is the axial direction along the pipe axis and Y is the vertical direction. In general, K_X will be different for axial and bending loads, in which case the component stresses are amplified (multiplied) by their respective K_X values prior to forming σ_X. For the sake of simplicity, the K_X values are the same in this problem:

(a) Determine the amplitude of the alternating and the mean (steady) *transverse* forces that the motor/fan exerts on the free end of the pipe:

$$\begin{array}{cc} \text{Alternating} & \text{Mean} \\[4pt] F_a^{\text{tip}} = \dfrac{3EI}{L^3} * \bar{\delta}_a^T & F_m^{\text{tip}} = \dfrac{3EI}{L^3} * \bar{\delta}_m^T \\[10pt] F_a^{\text{tip}} = 95.3\,\text{lb} & F_m^{\text{tip}} = 381\,\text{lb} \end{array} \tag{6}$$

(b) Determine the mean (steady) *axial* force and torque exerted by the wall on the pipe:

$$F_{\text{axial}} = \frac{EA}{L} * \delta_m^A = 957.2\,\text{lb}, \quad \Gamma = \frac{GJ}{L}\theta_m^A = 4068\,\text{in.lb} \tag{7}$$

(c) Determine the maximum *x* component of mean pipe stress including both bending and axial load contributions:

$$\sigma_m^{axial} = \frac{F_{axial}}{A}, \ \sigma_m^{bend} = \frac{M_m * D_0/2}{I}, \ \sigma_m^x = \sigma_m^{axial} + \sigma_m^{bend}, \ \sigma_m^x = 8250\,\text{psi} \tag{8}$$

(d) Determine the maximum *x* component of alternating pipe stress:

$$\sigma_a^{bend} = \frac{M_a * D_0/2}{I}, \ \sigma_a^x = \sigma_a^{bend}, \ \sigma_a^x = 1969\,\text{psi} \tag{9}$$

(e) Determine the pipe's mean shear stress at the wall:

$$\tau_m = \frac{\Gamma * D_0/2}{J}, \ \tau_m = 1050\,\text{psi} \tag{10}$$

(f) Determine the maximum von Mises, mean pipe stress:

$$\sigma_m' = \frac{1}{\sqrt{2}} \sqrt{2\left(K_X * \sigma_m^x\right)^2 + 6(\tau_m * K_{XY})^2}, \ \sigma_m' = 25016\,\text{psi} \tag{11}$$

(g) Determine the maximum von Mises, alternating pipe stress:

$$\sigma_a' = \sigma_a^x * K_X, \ \sigma_a' = 5906\,\text{psi} \tag{12}$$

(h) Determine the effective endurance limit "$S_{e,eff}$" at the wall where the above von Mises stresses occur:

$$S_{e,eff} = -\frac{S_e}{S_{ut}}\sigma_m' + S_e, \ S_{e,eff} = 18746 \tag{13}$$

Note that this is lower than the endurance limit ($S_e = 25000\,\text{psi}$) in the absence of a mean stress.

(i) What is the safety factor on the *vibration* amplitude $\bar{\delta}_a^T$ relative to the effective endurance limit, that is, what factor applied to $\bar{\delta}_a^T$ will cause the alternating von Mises stress to exceed the effective endurance limit "$S_{e,eff}$."

The alternating stress increases in proportion to $\bar{\delta}_a^T$; therefore, the factor on $\bar{\delta}_a^T$ to exceed $S_{e,eff}$ is

$$\frac{S_{e,eff}}{\sigma_a'} = 3.17$$

(j) Assume that the fan spins and the beam vibrates at $\omega = 100\,\text{rad/s}$. Also assume that the vibration amplitude on the fan bearing is the same as $\bar{\delta}_a^T$, and the supports are considered to be flexible. Provide a qualitative description of the vibration severity level. Provide a numerical justification for your answer.

The vibration velocity amplitude is $v = \omega\bar{\delta}_a^T$ so its rms value is

$$v_{rms} = \frac{\omega\bar{\delta}_a^T}{\sqrt{2}} = \frac{100 * 0.020}{\sqrt{2}} = 1.414\,\text{in./s} = 36\,\text{mm/s}$$

Table 1.4.4 shows this is an unacceptable level of v_{rms}.

Military standard MIL-STD-810D "Environmental Test Methods and Engineering Guidelines" provides guidance for inspectors and vendors of jet engine aircraft, propeller aircraft, and helicopters. Specifically, its objectives are:

(a) "To disclose deficiencies and defects and verify corrective actions"
(b) "To assess equipment suitability for its intended operational environment"
(c) "To verify contractual compliance"

Excessive vibration is considered to be potentially harmful due to the possibility of

- Wire chafing
- Loosening of fasteners
- Intermittent electrical content
- Touching and shorting of electrical parts
- Seal deformation (leakage)
- Component fatigue
- Optical misalignment
- Cracking and rupturing

Although these considerations concern mechanical distress, pilot fatigue is also a major concern. Standard MIL-STD-810D is a very comprehensive document, which contains a section on vibrations (section 514). Category 6 of section 514 considers helicopter vibration, which has a broadband random nature with strong sinusoidal vibrations due to onboard rotating machinery. This machinery includes engines, main and tail rotors, and meshing gears (transmission). The major peaks in the vibration spectrum are usually harmonics of the main rotor's blade-pass frequency (no. of blades ∗ main rotor spin frequency); however, different areas of the helicopter will have different sources at different frequencies as shown in Figure 1.4.11. The standard contains severity tables similar with Table 1.4.4 for various types of helicopters and general locations on the helicopters.

1.4.4   Machinery Productivity

Tool speed and depth of cut play a major role in productivity in machining and woodworking processes. Both of these factors are limited due to vibration. Chatter type vibrations result as the tool bit interacts with previously cut paths in milling, drilling, and boring operations. Suppressing these vibrations can yield a significant payoff in increased productivity.
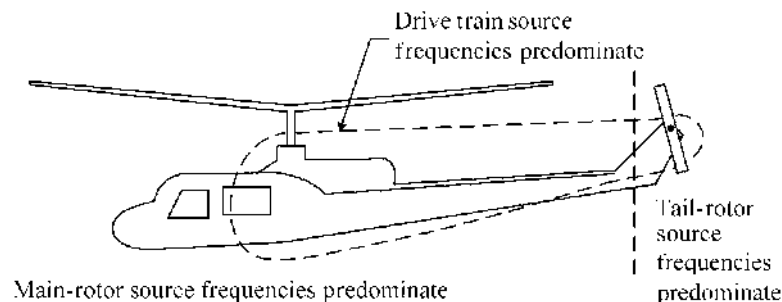

Figure 1.4.11 Helicopter dominant vibration zones

1.4.5   Fastener Looseness

Preloaded bolts (or nuts) rotate loose, when relative motion between the male and female threads takes place. This motion reduces the friction grip and permits the off-torque, which is proportional to the preload and thread pitch, to loosen the fastener. Transversely applied alternating forces generate the most severe condition for self-loosening. Appropriate choice of washers, installation of tie wires, and use of special bolts with more uniform load distributions between mating thread surfaces are some means to reduce bolt loosening. Attenuation of vibration treats this problem at its source. Fastener looseness is an especially important concern in high-performance machinery such as aircraft, helicopters, space shuttle, race cars, trains, roller coasters, and so on.

1.4.6   Optical Instrument Blurring

Lasers, telescopes, microscopes, interferometers, mirrors, and so on require a nearly vibration-free environment. This is typically accomplished by passive or active isolation of the equipment. Vibration has been called "the curse" in airplane- or helicopter-based aerial photography. Engine dynamic forces are transmitted through the airframe and into the camera resulting in blurry photos. High shutter speeds alleviate this problem at the expense of grainy photographs with less contrast. The camera must be soft mounted (isolated), which is more of a challenge for helicopter installations since the main rotor has a typically low frequency (e.g., ~30 Hz) and the camera must also be isolated from the tail rotor and engine frequencies (e.g., ~150 and ~250 Hz).

On the very small level, the lens-free AFM employs a tiny 100 μm length cantilever beam to measure local sample height (topography) at the atomic level. The beam has a very low spring stiffness (0.1 N/m) yet very high natural frequency. Mounted on the end of the cantilever is a sharp tip that is typically a 3 μm tall pyramid with 10–30 nm end radius. The deflection of the tip is measured with a laser. The beam and tip may also function in a noncontact mode where topographic images are derived from measurements of attractive forces. Environmental vibration can cause severe blurring of the topographic image produced by an AFM.

The space-based Hubble Space Telescope (HST) (Figure 1.4.12) experienced poor imaging due to vibrations of its original solar panels. The "jitter" interfered with operation
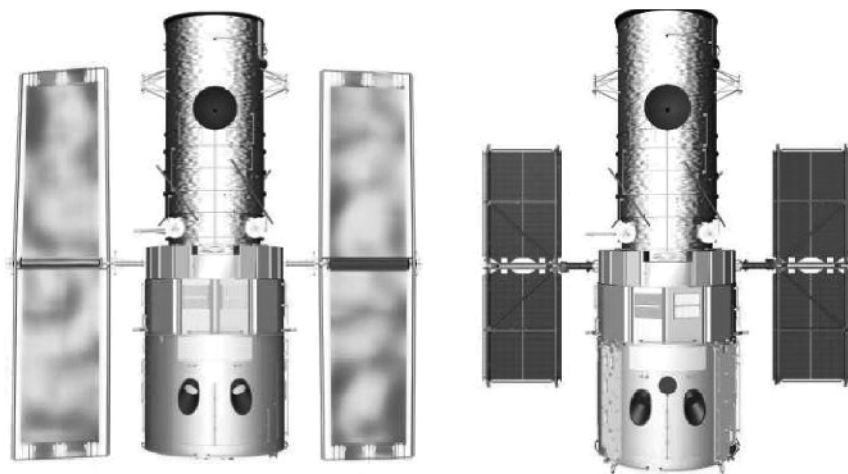
Figure 1.4.12 Hubble space-based telescope with original flexible and new rigid, smaller, and more powerful solar arrays.Reproduced with permission from NASA Goddard Space Flight Center

of the onboard optical instrumentation. The vibrations were induced by thermal deforma-tions resulting from its cyclic exposure to 45 minutes of searing heat and 45 minutes of frigid cold during every 90 minutes orbit around the earth. The transition from extreme hot to extreme cold occurs almost instantaneously subjecting the solar arrays to a transient thermal shock load in a very low vacuum. The vibration frequency of the arrays occurred at about 0.1 Hz (1 cycle/10 seconds).

1.4.7   Ethics and Professional Responsibility

Section **1.4** has stressed some practical aspects of vibrations and why they should be tamed. I once heard a person say "why worry about standards, there are not the law." This is true however from a commercial and sometimes litigation standpoint they have very high impor-tance. It may be quite difficult to sell a machine that vibrates in excess of the limits defined by the standards during commissioning of the machine to industry or government users. Similarly, it may be challenging to defend operation of a machine prior to failure that may have resulted in loss of millions of dollars of products, facility damage, injury, or even death, if vibrations were related to the failure and the operating vibrations exceeded the lim-its provided in the standards. Insurance companies which pay for failures and accidents and judicial arbiters view industry and government standards with great seriousness, sometimes even more so than arguments based on detailed testing or simulation model results.

1.4.8   Lifelong Learning Opportunities

The list of vibration standards and related materials is very long and includes documents from many countries. A web search at the time of the writing of this book identified the following:

(a) International Organization for Standardization (ISO—130 member countries)
   http://www.iso.org/iso/home/store/catalogue_ics.htm (search vibration)
(b) US Military Standards (MIL)
   http://quicksearch.dla.mil/ (search vibration)
(c) UK Health and Safety Executive
   www.hse.gov.uk/index.htm (search vibration)
(d) American Petroleum Institute (API)
   http://www.api.org/Standards/

This large number of standards is just one example of the fact that it is truly a lifelong learning experience to be a vibrations expert.

1.5   STIFFNESS, INERTIA, AND DAMPING FORCES

Systems vibrate due to the interplay (energy exchange) between *stiffness* (restoring), *inertia* (mass), and *damping* (drag) related forces. Figure 1.5.1 shows the top view of a horizontal spring/mass/damper system. The deflection of the spring in Figure 1.5.1(a) would always be

$$x(t) = \frac{F(t)}{k} \tag{1.5.1}$$

in a world without mass. This follows from *Newton's second law* (with mass = 0) and the spring's force–deflection relation. Equation 1.5.1 shows that point p will vibrate (oscillate) only if the external force F is oscillatory (periodic). Experience reveals that real systems oscillate even in the absence of oscillatory external forces, that is, the occurrence of natural
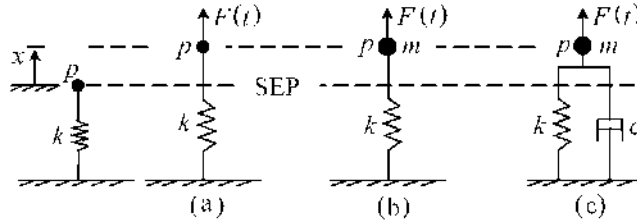
Figure 1.5.1 Response of spring/mass/damper system to external force $F(t)$

vibrations or vibrations due to a nonperiodic force. To understand why, consider the following discussion.

The spring stiffness acts to pull point p back toward its *static equilibrium position (SEP)*. In fact, if k became infinite, it would pull x to the SEP independent of a finite valued $F(t)$. Equation (1.5.1) implies that

$$x = \begin{cases} F_0/k, & F(t) = F_0 \\ 0, & F(t) = 0 \end{cases} \tag{1.5.2}$$

so that x would instantaneously become zero at the moment $F(t)$ was removed. Suppose a mass is now attached to point p as shown in Figure 1.5.1(b). This mass will deflect by $x_0 = F_0/k$ if $F(t)$ is pseudostatically increased from zero to F_0. Should the response in (1.5.2) still be expected if F_0 is suddenly removed with m attached? Intuition tells us no for several reasons:

(a) The spring has potential energy $\left(\text{PE} = (1/2)kx_0^2\right)$ when deflected at $x = x_0$. If x becomes zero, its P.E. is zero. Where did the potential energy go? The answer is kinetic energy, which implies that $\dot{x}(t)$ is not equal to zero at $x = 0$.

(b) By (a) m has velocity $(-v_0)$, that is, momentum as it passes through $x = 0$ at $t = t_0$. The spring force needs time to change the momentum of m from zero at $x = x_0$ to $-mv_0$ at $x = 0$. This results from the *impulse and momentum theorem*

$$I_k = \text{impulse on } m \text{ from spring } k = \int_0^{t_0} -kxdt = \Delta(mv) = m\Delta v = -mv_0 \tag{1.5.3}$$

Thus, x cannot return to zero instantaneously as was the case with no mass m in (1.5.2). The spring force exerts a positive impulse as soon as x becomes less than zero so m begins to decelerate. This implies that v_0 is the maximum velocity of m. The potential energy of the spring will become $(1/2)kx_0^2$ at $x = -x_0$. Therefore, the mass must have zero *kinetic energy* at $x = -x_0$ by conservation of energy, so its velocity is zero. The spring's impulse increases and m's velocity again becomes positive. In this manner, the impulse of the spring force periodically changes $m's$ momentum (velocity direction) alternately positive and negative. This is the mechanism of free vibration. Both k and m influence the period of free vibration as can be seen from Equation (1.5.3).

The *work* performed on m by the damper in Figure 1.5.1(c) is negative since

$$W_c = \int_{x_1}^{x_2} F_c dx = \int_{t_1}^{t_2} -c\dot{x}\ddot{x}dt = -c\int_{t_1}^{t_2} \dot{x}^2 dt < 0 \tag{1.5.4}$$

Energy is therefore removed from the system by damper c and the vibration diminishes to zero. This diminution to zero will not occur if another external force performs positive work on the system.
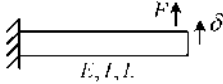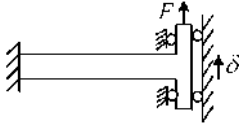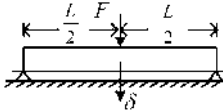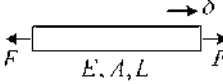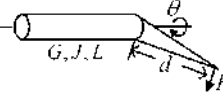
The word stiffness typically invokes an image of a coil spring that may deform in stretch or compression creating a force or in torsion creating a torque. Ultrahigh-strength springs as shown in Figure 1.5.2 are used in a myriad of machinery, instrument, transportation, and/or other applications.

In general, stiffness results from the restoring force capability of strain energy in a deformed elastic object. Table 1.5.1 shows an assortment of typical stiffness elements.
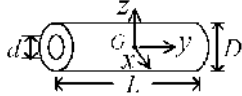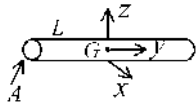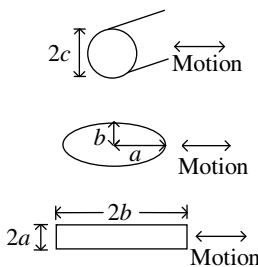

Figure 1.5.2 Assortment of extension–compression and torsion springs. Reproduced with permission from Murphy & Read Spring Manufacturing Co.

Table 1.5.1   Assorted stiffness elements

Entry	Description	Figure	Stiffness
1	Free cantilever		$k = \dfrac{F}{\delta} = 3\dfrac{EI}{L^3}$
2	Guided cantilever (zero rotation at tip)		$k = \dfrac{F}{\delta} = 12\dfrac{EI}{L^3}$
3	Simply supported beam		$k = \dfrac{F}{\delta} = 48\dfrac{EI}{L^3}$
4	Coiled spring (round wire) G = shear modulus N = number of coils		$k = \dfrac{F}{\delta} = \dfrac{Gd^4}{8D^3N}$
5	Stretched rod		$k = \dfrac{F}{\delta} = \dfrac{EA}{L}$
6	Torsion spring G = shear modulus J = torsion constant		$k_{\mathrm{T}} = \dfrac{Fd}{\theta} = \dfrac{GJ}{L}$

Table 1.5.2   Assorted mass elements

Entry	Description	Figure	Inertia
1	Hollow cylinder ρ = mass density G = mass center		$m = \dfrac{\rho \pi L (D^2 - d^2)}{4}$ $I_y = \dfrac{m}{8}\left(D^2 + d^2\right)$ $I_x = I_z = m\left(\dfrac{L^2}{12} + \dfrac{(D^2 + d^2)}{16}\right)$
2	Long slender rod G = mass center		$m = AL\rho$ $I_x = I_z = \dfrac{mL^2}{12}$
3	Vibration of soil in liquid ρ = density of liquid	Cross-sections 	Added mass per unit length $\rho \pi c^2$ $\rho \pi b^2$ $1.15\, \rho \pi a^2,\ (a = b)$ $1.14\, \rho \pi a^2,\ (a = 10b)$

Likewise, Tables 1.5.2 and 1.5.3 show assortments of mass and damping elements. Finally, Table 1.5.4 shows a table of force expressions.

The following analysis shows a derivation of entry 2 (Table 1.5.3). A liquid flowing with velocity u and laminar Reynolds (R_e) number ($(\rho u d_H)/\mu$) experiences the pressure drop

$$\Delta p = \rho \frac{L}{d_H} \frac{u^2}{2} f \qquad (1.5.5)$$

as it flows through a pipe of length L. The laminar flow friction factor may be obtained from most fluid mechanics text as

$$f = \frac{64}{R_e} = \frac{64\mu}{u d_H \rho} \qquad (1.5.6)$$

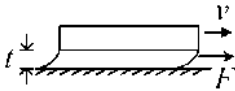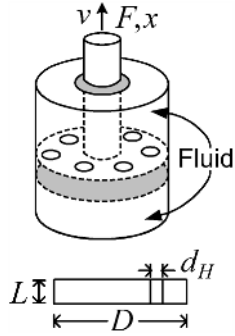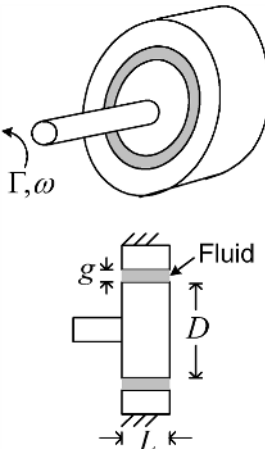Substitute (1.5.6) into (1.5.5) to obtain

$$\Delta p = 32 \frac{L \mu u}{d_H^2} \qquad (1.5.7)$$

Let A be the entire area of the piston and "a" the area of a single hole. Then the time rate of change of the upper volume is

$$\frac{\Delta V}{\Delta t} = vA = \frac{\Delta x}{\Delta t} A \qquad (1.5.8)$$

Table 1.5.3   Assorted damping elements

Entry	Description	Figure	Damping
1	Parallel plate damper $A =$ plate wetted area $\mu =$ absolute viscosity		$C = \dfrac{F}{v} = \dfrac{\mu A}{t}$
2	Orifice damper $\mu =$ fluid absolute viscosity $n =$ no. of orifice holes		$C = \dfrac{F}{v} = \dfrac{8\pi L\mu}{n}\left(\dfrac{D}{d_H}\right)^4$
3	Torsional damper $\mu =$ fluid absolute viscosity		$C_T = \dfrac{\Gamma}{\omega} = \dfrac{2\pi\mu L D^3}{8g}$

The volumetric flow rate through the n holes is

$$Q_H = nua \tag{1.5.9}$$

Conservation of the mass for an incompressible liquid requires that

$$Q_H = \frac{\Delta V}{\Delta t} \Rightarrow u = \frac{vA}{n\,a} = \frac{v}{n}\cdot\frac{\pi D^2/4}{\pi d_H^2/4} = \frac{v}{n}\left(\frac{D}{d_H}\right)^2 \tag{1.5.10}$$
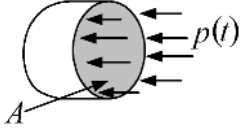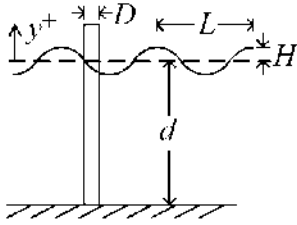
Substitute (1.5.10) into (1.5.7)

$$\Delta p = \frac{32 L\mu}{d_H^2}\frac{v}{n}\frac{D^2}{d_H^2} \tag{1.5.11}$$

The net force on the piston is

$$F = \Delta p A = \frac{\pi D^2}{4}\Delta p \tag{1.5.12}$$

Table 1.5.4 Assorted force expressions

Entry	Description	Figure	Force
1	Pressure force		$F(t) = pA(t)$
2	Wave force on circular cylinder		$F(y,t) = $ force per unit length
	$T = $ wave period		$= g_1(y)g_2\left(\dfrac{\pi D}{L}\right) * \cos(\omega t - g_3)$
			$g_1(y) = \dfrac{2\rho g H}{k}\dfrac{\cosh(k(d+y))}{\cosh(kd)}$
	$\omega = $ wave frequency $= 2\pi/T$		$g_2\left(\dfrac{\pi D}{L}\right) = \left\{\left[J_1'\left(\dfrac{\pi D}{L}\right)\right]^2 + \left[Y_1'\left(\dfrac{\pi D}{L}\right)\right]^2\right\}^{-1/2}$
	$k = $ wave frequency $= 2\pi/L$		$g_3 = \tan^{-1}\left(\dfrac{J_1'\left(\dfrac{\pi D}{L}\right)}{Y_1'\left(\dfrac{\pi D}{L}\right)}\right)$
	$\rho = $ mass density of water		$J_1' = $ derivative of the first order Bessel function of the first kind
	$g = $ gravity constant		$Y_1' = $ derivative of the second order Bessel function of the second kind

if $na << A$. Insert (1.5.11) into (1.5.12) to obtain

$$F = cv \tag{1.5.13}$$

where

$$c = \frac{8L\mu\pi}{n}\left(\frac{D}{d_H}\right)^4 \tag{1.5.14}$$

1.6 APPROACHES FOR OBTAINING THE DIFFERENTIAL EQUATIONS OF MOTION

The equations of motion for a vibrating system model provide a starting point for simulating the system's response to initial conditions, external forces, or parametric excitation (time-dependent system parameters). Approaches for deriving the equations of motion for a model of a vibrating system are discussed below.

(a) *Newton's Laws (Chapter 3)*
These laws represent the balance between external and inertial forces as first proposed by Sir Isaac Newton. Practical applications required extension of this balance from a particle to a collection of particles and finally to a rigid body. The translational and rotational forms of Newton's laws for rigid bodies are presented in Chapter 3.

(b) *The Power Conservation Approach (Chapter 4)*

Applying power conservation for deriving the equations of motion has a physical intuition appeal. The potential and kinetic energy expressions form the starting point for applying the method. This approach has an advantage of being able to disregard all forces that perform a net work of zero, as discussed in Chapter 4.

(c) *The Lagrange–Hamilton Approach (Chapter 4)*

The Lagrange–Hamilton approach utilizes expressions for kinetic and potential energy to develop the equations of motion for the system. This approach may be interpreted as a restatement of Newton's laws or an entirely different physical principle based on making an "action" integral stationary, using the calculus of variations.

   The Lagrange approach for formulating the equations of motion of a rigid or flexible body model circumvents some tasks for direct application of Newton's law. These include:

- No direct evaluation of acceleration vectors for the mass center(s)
- Less applications of Newton's third law for equal and opposite reactions in many instances
- Less sign determination for many forces
- Direct use of potential energy to evaluate internal force effects in a flexible body
- Direct means to formulate equations of motion in terms of any generalized coordinate, which may consist of an actual physical coordinate or of a parameter that governs a distributed shape for deflections (this is a key capability in the assumed modes and finite element methods)

The Lagrange approach is discussed extensively in Chapter 4.

1.7   FINITE ELEMENT METHOD

The finite element method (FEM) is widely used in industry for avoiding machinery and structural vibration problems. User-friendly graphically driven interfaces have greatly facilitated the efficient use of this method. Direct conversion of solid modeler geometry descriptions into finite element "meshes" is quickly becoming standard practice for the simulation of vibrations of components and systems of all sizes and shapes. This is illustrated in Figure 1.7.1.

   The meshes consist of discrete node points that define finite-sized subvolumes referred to as elements. The motions within any element are approximated by interpolation functions, which interpolate the displacements at the node points throughout the element. The interpolation functions are generally linear or quadratic functions of position but may be more complex as a result of "isoparametric" transformations that enable the element to possess general 2- or 3-dimensional shapes. The FEM has its theoretical foundations in the more general areas of energy principles and weighted residual methods. The former utilizes the variational approach of determining the solution of the equilibrium equations by finding solutions that make a companion functional stationary (maximum or minimum), as in the case of the principle of virtual work, Hamilton's principle, or the principle of minimum total potential energy. The latter develops a "weak" form of the original equilibrium equations by integrating products of weight functions times the equilibrium equations while lowering continuity requirements on the interpolation functions utilizing integration by parts (divergence theorem). The net result is typically a very large order system of linear differential equations that are numerically integrated to obtain the time-varying displacements at the node points. These displacements can then be utilized to solve for stresses, which are in
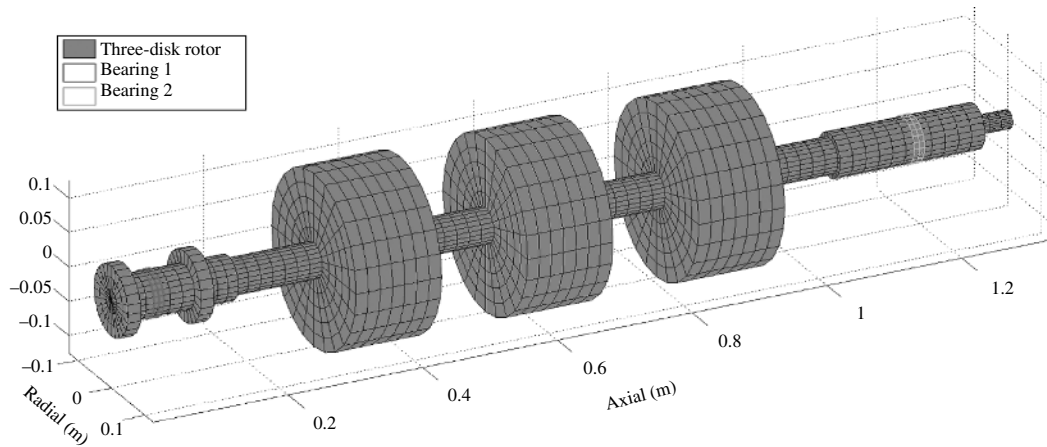
Figure 1.7.1 Finite element mesh generated from a solid model of a shaft
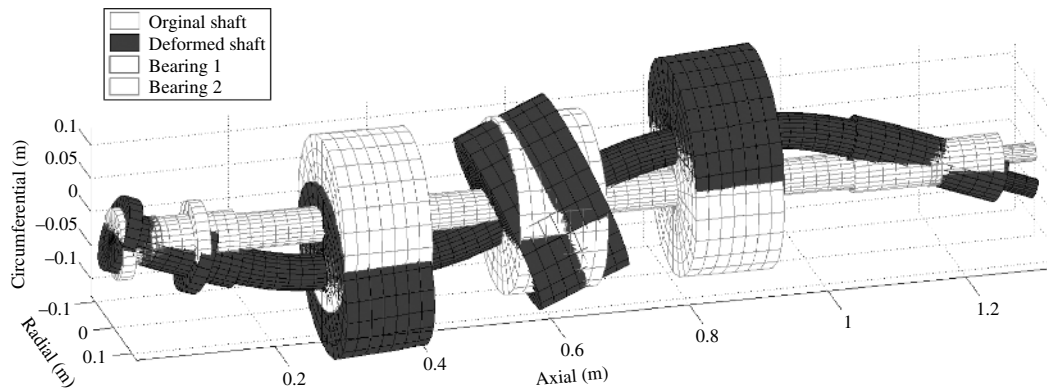

Figure 1.7.2 Vibration "mode shape" obtained from a finite element model

turn utilized to predict fatigue life. The system of equations can also be solved to obtain eigenvalues and eigenvectors, which describe the "mode" shapes and "natural" frequencies of the modeled system in free (unforced) vibration. This is illustrated in Figure 1.7.2 for the finite element model in Figure 1.7.1.

So why study finite element theory when its application tools are quickly progressing toward a nearly automated state? There are several very good reasons, including:

(a) Cost: The "honeymoon is over" as far as cheap software when one leaves the university and enters industry or private practice. Single seat, annual licensing fees in the tens of thousands of dollar range for industrial users are common.

(b) Proper usage of commercial software (CS): CS can be easily misused by not understanding the limitations (assumptions) of the theory implemented by the CS. Understanding the theory will guide one to utilize the appropriate software options and avoid the ineffective ones.

(c) Advancement and customization: Engineering technology is advancing at an incredible rate requiring the use of novel materials, smart and multidisciplinary systems, newly

discovered empirical force descriptions, and so on. CS sometimes lags behind these needs requiring engineers to develop their own finite element software. Customer input and output requirements may also motivate engineers to develop their own finite element software.

(d) General innovation: Who knows what new methods of modeling and simulation lies over the horizon? It's hard to say, however, chances are good that it will build on the theory of existing methods. Knowledge of finite element theory will provide a foothold to reach out and develop new theoretical approaches for simulation.

The book provides the necessary theory and implementation tools required to develop your own finite element codes. The progression of element sophistication is ordered from simple spring mass systems to general 3D solids in the book to facilitate comprehension and to provide results of significant practical value.

1.8   ACTIVE VIBRATION CONTROL

Passive vibration control seeks to achieve vibration mitigation goals via structural modification and installation of devices such as absorber masses, spring, and dampers to reduce the system sensitivity to external disturbances and to self-excitation forces, that is, instability. Passive devices have limits though in adaptability and environmental operating conditions. Active vibration control AVC devices can replicate the behavior of a passive device as described and also produce forces with a more general dependence on motion variables. AVC devices may also adapt to changing operating condition variables and function well even in extreme temperature and pressure environments, including vacuum conditions. Chapter 12 provides an in-depth introduction to the methodology of AVC. This includes discussions of modeling methods, common architecture, simulation and solution procedures, and analysis of electromagnetic and piezoelectric actuators.

1.9   CHAPTER 1 EXERCISES

1.9.1   Exercise Location

All exercises may be conveniently viewed and downloaded at the following website: **www.wiley.com/go/palazzolo**. This new feature greatly reduces the length of the printed book, yielding a significant cost savings for the college student and allows the author to provide additional exercises.

1.9.2   Exercise Goals

The goal of the Exercises in Chapter 1 is to strengthen the student's understanding and related engineering problem-solving skills in the following areas:

(a) The presence of vibrations in natural and industrial processes and devices

(b) The deleterious effects of vibration on the reliability, efficiency, and safety of industrial processes and devices and on human health

(c) The quantified descriptions of vibrations

(d) The determination of failure and life of a vibrating object

(e) The use of vibration standards established by industry and government

1.9.3   Sample Exercises: 1.6 and 1.11

Exercise 1.6 illustrates the use of machinery vibration standards for multiharmonic vibrations of an electric motor-driven pump. Exercise 1.11 considers a vibrating, pulsation suppression vessel for a natural gas transmission compressor. This exercise requires evaluation of component and von Mises (equivalent) stresses and component life, given mean and alternating (vibrating) motions. This exercise should impress on the student the role that vibration analysis plays in designing machines for greater reliability and sharpen skills in fatigue-related failure.
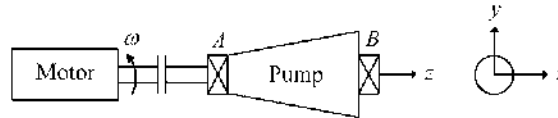
(1.6)
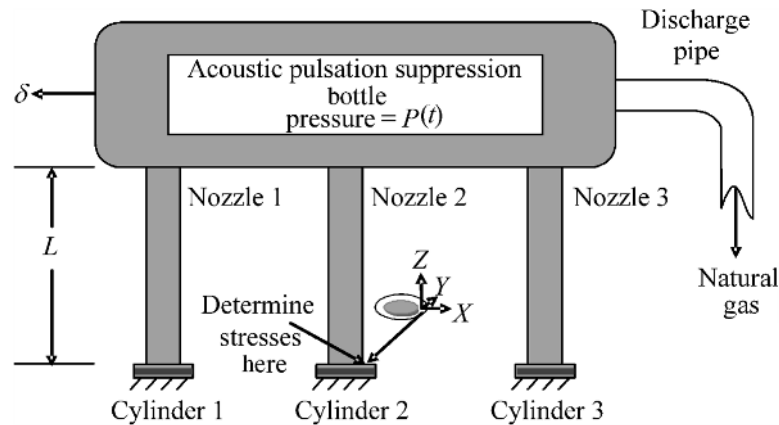
(1.11)

REFERENCES

ASTM E-1049–85, *Standard Practices for Cycle Counting in Fatigue Analysis*, (Reapproved 2011), http://www.astm.org/DownloadStandardB.html?ASTM%20HC=ASTM&DESIGNATION= E1049&AdID=&Split=&Campaign=Individual%20Standards%207&gclid=COf9kujhlcgCFYM-aQodJ5cD4w (accessed 15 October 2015).

BUDYNAS, R. and NISBETT, J., *Shigley's Mechanical Engineering Design*, 8th ed., McGraw Hill, New York, 2008.

CANNON, R. H., *Dynamics of Physical System*, 1st ed., McGraw Hill, New York, 1967.

CDC, *Health Hazard Report No. 94-0425*, 1994.

COLLINS, J. A., *Failure of Materials in Mechanical Design*, 1st ed., John Wiley & Sons, New York, 1981.

GRIFFIN, M. J., *Handbook of Human Vibration*, 1st ed., Academic Press, London, 1990.

HASSAN, O. A. B., *Building Acoustics and Vibrations*, 1st ed., World Scientific Publishing, Singapore, 2009.

LEE, Y.-L., BARKEY, M. E., and KANG, H. T., *Metal Fatigue Analysis Handbook: Practical Problem-Solving Techniques for Computer-Aided Engineering*, Elsevier, Waltham, MA, 2012.

NEWMAN, CARDINAL, J. H., *The Idea of a University*, edited by D. M. O'Connell, Loyola University Press, Chicago, IL, 1927.

NICHOLAS, T., *High Cycle Fatigue: A Mechanics of Materials Perspective*, Elsevier, Oxford, 2006.

NIESLONY, A., *Rainflow Counting Algorithm*, MATLAB, Mathworks, Inc., Natick, MA, 2010.

NIOSH, *Occupational Exposure to Hand-Arm Vibration*, US Department of Health and Human Services, Cincinnati, OH, 1989. http://www.cdc.gov/niosh/docs/89-106/89-106.pdf. Accessed August 4, 2015.

PILKEY, W. D., *Peterson's Stress Concentration Factors*, 2nd ed., John Wiley & Sons, Inc., New York, 1997.

SHIGLEY, J. E., *Mechanical Engineering Design*, McGraw Hill, New York, 1989.

WANG, S., Mean Shear Stress Effect for a Notch-Free Ductile Material Under Pure Cyclic Torsional Loads, *Journal of Pressure Vessel Technology*, Vol. **128**, pp. 667–669, 2006.